Spatio-Temporal Variability Assessment and Frequency Analysis of Precipitation over Northern Regions of Pakistan

By

Mukarrma Anwar

(2018-NUST-MS-GIS-276227)

A thesis submitted in partial fulfillment of the requirements for the degree of Master of Science in Remote Sensing and GIS

Institute of Geographical Information Systems
School of Civil and Environmental Engineering
National University of Sciences and Technology
Islamabad, Pakistan
August 2022

CERTIFICATE

Certified that the contents and form of thesis entitled **Spatio-Temporal Variability Assessment and Frequency Analysis of Precipitation over Northern Regions of Pakistan** submitted by Ms. Mukarrma Anwar (Registration No. 2018-NUST-MS-RS&GIS-276227) has been found satisfactory for the requirements of Master of Science degree in Geographical Information Systems and Remote Sensing.

Supervisor: _____

Dr. Muhammad Azmat

IGIS, NUST

Member: _____

Dr. Ejaz Hassan

Professor

IGIS - SCEE, NUST

Member: _____

Dr. Salman Atif

Assistant Professor

IGIS - SCEE, NUST

Member: _____

Dr. Zamir Hussain

Assistant Professor

SINES, NUST

DEDICATION

To

My Sweet & Loving Family

Thanks for their love, care, and motivation all the way since the start of my studies, and to all those who encouraged me and prayed for me for the completion of this thesis.

ACADEMIC THESIS: DECLARATION OF AUTHORSHIP

I, Mukarrma Anwar declare that this thesis and the work presented in it are my own and have been generated by me as the result of my own original research.

Spatio-Temporal Variability Assessment and Frequency Analysis of Precipitation over Northern Regions of Pakistan

I confirm that:

1. This work was done wholly by me in candidature for an MS research degree at the National University of Sciences and Technology, Islamabad.
2. Wherever I have consulted the published work of others, it has been clearly attributed.
3. Wherever I have quoted from the work of others, the source has been always cited.
4. I have acknowledged all main sources of help.
5. Where the work of thesis is based on work done by myself jointly with others, I have made clear exactly what was done by others and what I have contributed myself.
6. None of this work has been published before submission. This work is not plagiarized under the HEC plagiarism policy.

Signed: ……

Date: ……

ACKNOWLEDGEMENTS

All praises to Allah Almighty, and blessings upon Prophet Muhammad (peace be upon him). I owe my sincere gratitude and pleasure to my respected research supervisor Dr. Muhammad Azmat, for his devoted guidance and encouraging attitude throughout the research. I am also grateful to guidance and examination committee members, for their coordination. This research would have not been possible without the sincere cooperation and consistent support of IGIS NUST, which supported me in all activities. It is a pleasure to pay tribute to all my sincere friends, colleagues, and family members, particularly my parents for their sincere attitude, support, patience, and prayers which inspired me every moment towards successful completion of my tasks.

TABLE OF CONTENT

LIST OF FIGURES

LIST OF TABLES

ABSTRACT

The hydro-meteorological factors of excessive rainfall are difficult to explain because of unexpected changes in climate and varying water demand as the population grows. The study aims to improve comprehension of the frequency and magnitude of total precipitation with the help of recent techniques and providing practical knowledge in making development strategies for water resource management in one of Pakistan's most significant climatic regions. For that purpose, spatio-temporal rainfall variability, trends analysis, and regional rainfall frequency analysis for multiple meteorological stations in Gilgit Baltistan are performed. The data of precipitation is acquired from Pakistan Meteorological Department spanning 1990 to 2020. Temporal and spatial trend analysis are performed using Man Kendall test and Sen's Slope technique and linear moments technique are utilized to calculate regional frequency analysis. For regional frequency analysis data series are random, independent and identical distributed, and no site is discordant in the region. The selection of distribution is done by methods of L-moments ratio diagram and Z-statistics. Generalized Pareto Distribution (GPA) is appeared to be the most suitable distribution to represent the statistical properties of precipitation data. The results show that the station of Astore, Hushey and Khunjerab have observed annual trends. Astore has experienced a decreasing trend of 186 mm of rainfall whereas Khunjerab and Hushey have experienced an increasing trend of 230 mm and 252 mm over last three decades. Some of the stations have also experienced seasonal trends. Moreover, most of the stations have not observed any significant trends in rainfall. The results of regional frequency analysis have shown that the stations of Astore, Naltar, Rattu, Rama, Khunjerab and Hushey are at higher risk of observing extreme rainfall events 100 years return period event in any of coming year. The study could help in hydrological planning and irrigation water resources management, and in policy making in disaster prevention and mitigation.

Chapter 1

INTRODUCTION

1.1 Global Warming and Cascading Effect

Human-induced global rise in mean temperature has come to around 1°C (likely between 0.8°C and 1.2°C) over pre-industrial levels in 2017, increasing at 0.2°C (likely between 0.1°C and 0.3°C) per decade (Hoegh-Guldberg et al., 2018). Human-caused global warming has already resulted in a number of observable alterations in the climate system i.e., changes in land and ocean temperatures, more frequent heatwaves, extreme precipitation events and increased risk of droughts. Trends in the intensity and frequency of various climate and weather extremes have been seen throughout time periods of around 1°C global warming compared to pre-industrial age. Moreover, the future projections of temperature and precipitation also indicate that dry and wet events significantly increase in their magnitude and frequency globally (Aihaiti et al., 2021)

Climate change is a change in the condition of climate, which can determine by changes in the mean of its attributes over an extended period, generally decades or longer (IPCC 2022). The four key climate indicators that have set new records in 2021 are greenhouse gas concentration, sea-level rise, ocean heat, and ocean acidification (Trewin et al., 2021). IPCC 2022 reported that the world would reach a 1.5ºC level within two decades. According to the World Meteorological Organization global climate report 2022, the past seven years have been the warmest. Climate changes have been intensified since late 20^{th} century due to anthropogenic activities, fossil fuel burning, and greenhouse gases that raise the earth's surface temperature. Evidence shows that climate change will have adverse effects like extreme temperatures, seasonal shift in precipitation patterns, increased frequency of extreme precipitation events, sea-level rise, and heat waves (Lawrence et al., 2020).

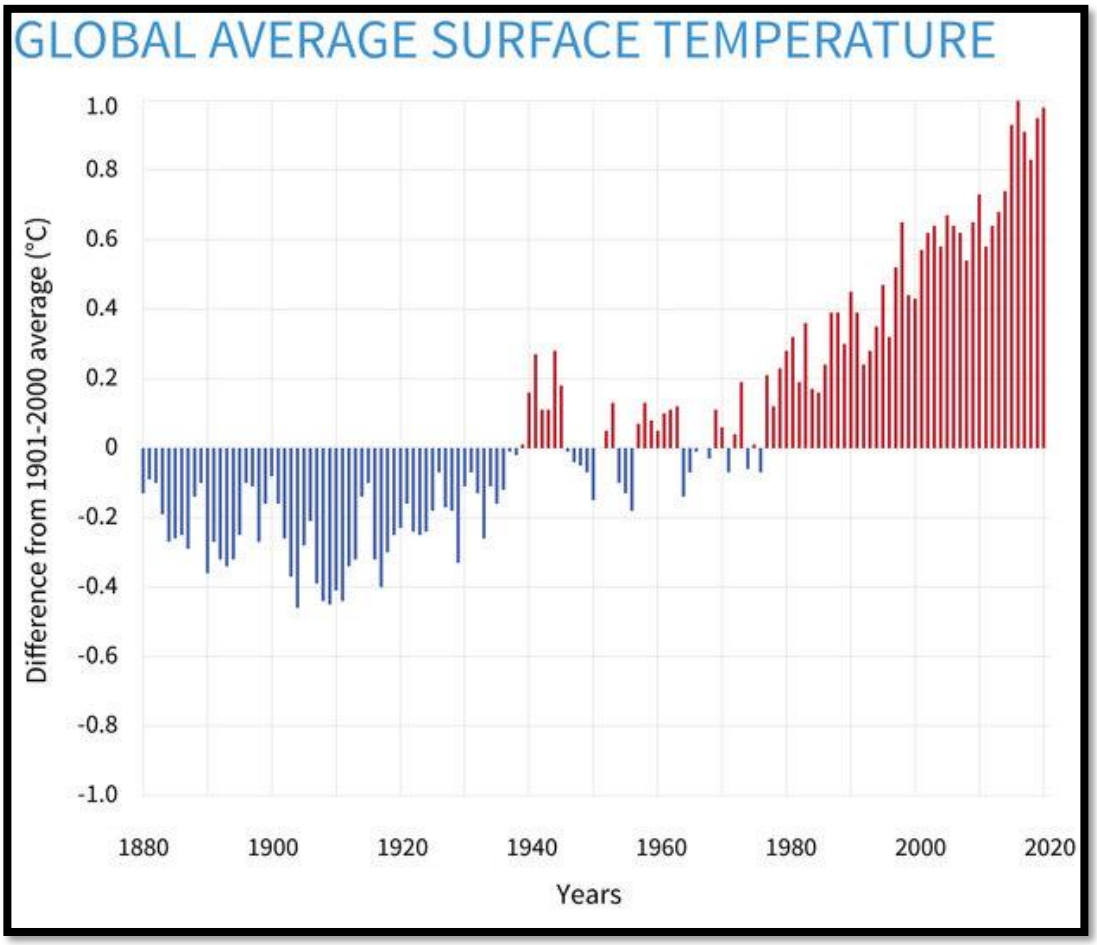

Fig. 1.1 Average difference in global temperature from 1880-2020.

1.2 Climate Change Effects on Precipitation Patterns

Global warming causes higher concentration of atmospheric water vapor, which supplies the water for precipitation, as it rises in proportion to saturation at a rate of around 6–7 percent per degree of temperature rise (Tabari, 2020). Because of that extreme precipitation is anticipated to intensify globally and locally. Moreover, current climatic models have also indicated that an increase in temperatures will result in intense precipitation as a result, extreme rainfall events and the floods are expected (Trenberth, 2011). Further, studies have statistically proven the increasing presence of trends in precipitation patterns. A trend is an increasing or decreasing shift in a climatic parameter. Hence, there is significant evidence that changes in rainfall patterns have already occurred on both global and regional dimensions as a result of global warming. Variations in regional and local climate are influenced by regional and local characteristics; as a result, climate change on a regional and local scale frequently differs from that on a worldwide one. In this respect, assessing climate variability and change on a smaller scale (at the nation level) is critical, as it aids in our knowledge of long-term climate variability and change, as well as the related processes of change forcing at the country or local scales (Rahman & Lateh, 2017).

1.3 Climate Change in Gilgit Baltistan

Generally, underdeveloped countries are more prone to the consequences of climate change than developed ones, owing to the developing world's limited ability to adapt to change. Like global climate change, Pakistan's climate is changing, becoming more unpredictable in recent years. Pakistan, like many other countries, will confront enormous problems from climate change, especially given that Pakistan has agrarian economy with a large population. As a result, climate change scenarios must be integrated into the country's renovation and planning operations, as agriculture and water are the most effected historically by alterations in climatic patterns, which can result in floods, droughts, cyclones, soil salinity and other

meteorological disasters. According to the report of "Gilgit Baltistan Climate Change Strategy and Action Plan ", an increase of 0.15°C per decade in average temperature and -4.3 mm per decade in average rainfall at five weather stations from 1984 – 2012 (Shehzad Hasan Shigri, 2017).

Gilgit Baltistan being the northern region of Pakistan embodies some of the world longest and highest mountain ranges i.e., Himalayas, Karakoram and Hindu Kush, and the freshwater reservoir in the form of glaciers, making GB the most significant climatic region for country. Research shows that the temperature of the region is rising at a rate twice than that of the plains. Because of its delicate mountain ecology, terrain, geological composition, and geographic location, as well as its dispersed population and socioeconomic situations (Shehzad Hasan Shigri, 2017).

1.4 Frequency Analysis

Pakistan has experienced natural calamities most common among them are floods, droughts, and storms. These enormous disasters occur naturally and cannot be totally avoided. Although, with appropriate preparation, the losses might be reduced to some extent. Most of the disasters are related to unpredictable total maxima precipitation events. Estimates of extreme precipitation events such as the 100-year flood or rainfall event are frequently required in the construction of water resources infrastructure like spillways, storm surge barriers and dams, and irrigation water management. Hence, along with the quantitative study to measure the changing trends and variability in precipitation, the estimation of magnitude and frequency of precipitation events is of utmost importance as extreme precipitation events are one of the most disastrous hydrometeorological events. In economically developing countries like Pakistan, since the length of recorded data for the variable of interest is usually only approximately 30 to 50 years, estimating the annual extreme occurrences directly from the data

is often not practical, and such severe rainfall occurrences are extrapolated via frequency analysis.

Frequency analysis has been done typically in past. This analysis is the estimation of how frequently the event of same magnitude will take place again. The method of frequency analysis involves fitting a frequency model to the observed data. Several statistical and probabilistic techniques are used in their estimation. The methods for fitting statistical distributions to sample data, including graphical approaches, methods of moments, maximum likelihood, least square, probability weighted moments etc. As compared to these conventional methods of regional frequency analysis in practice, the approach based on Linear moments has many reported benefits i.e., its efficiency is not affected by smaller sample size and it has no assumption of data structure.

The L-moments approach corresponds linear combination of sample data to corresponding theoretical formulations using statistical distribution parameters, in order to specify distribution parameters, that is similar to the probability weighted moments approach. Conventional moments, raise raw data to powers of 2, 3, and 4, with higher order moments. L-moments avoid non-linear transformations of data because they can lead to distortions and thus poor parameter estimates when there are outliers or extreme values in the data (Pearson, 1991).

In this research, regional frequency analysis is done for annual monthly totals rainfall (AMTR) in the northern regions of Pakistan utilizing the index flood approach of employing L-moments established by Hosking (1990) to overcome the lack of data and model uncertainty. The basic procedure of frequency analysis includes calculation of linear moments from time series data. The recognition of homogenous region is done using heterogeneity test, of region of interest turns out to be non-homogeneous then the smaller homogeneous regions are made with the help of cluster analysis. The selected distributions are tested for best suited frequency

distribution for our data, based on different graphical and statistical techniques, estimation of distribution parameters is done and prediction of regional and at stations quantiles have been made.

1.5 Objectives and significance of study

The study aims to analyze statistical and spatial of rainfall data during 1990 to 2020 in context of trends, variability and spatial patterns, on the annual and seasonal basis. And to estimate regional and at-site quantiles of total precipitation of Gilgit Baltistan at both short and long return periods.

Since, Gilgit Baltistan is susceptible to the climate change i.e. changing seasonal patterns, changing agricultural patterns, spatial and temporal changes in precipitation, increasing frequency of hydro-meteorological disasters, and shrinking glaciers (Shehzad Hasan Shigri, 2017). This climate change is anticipated to have far-reaching consequences not just for the Gilgit Baltistan, but also for mainland populations that rely significantly on mountain water for household, agricultural, energy, and industrial needs. The agriculture calendar might be thrown off by seasonal changes in precipitation and rising temperatures (Mass Awareness & Understanding of Climate Change in Gilgit-Baltistan, 2017).

Trend analysis, the method of determining spatial and temporal variations for various parameters associated with climate is of utmost importance in understanding long term climate variability and the related processes of change forcing like meteorological disasters at country and local levels (Swain et al., 2015). The results of frequency analysis are useful in irrigation water management and flood disaster prevention measures in Gilgit Baltistan. The results of this study could be employed by researchers, scientists, hydrologists, government authorities for flood disaster prevention, agricultural water management, and improvement projects for main barrages, Dams and spillways renovation.

Chapter 2

LITERATURE REVIEW

2.1 Rainfall Trends and Variability Analysis

Hussain et al. (2021) assessed the spatiotemporal rainfall variability across Pakistan's sub-Himalayan Pothwar region's, Soan River Basin (SRB). using data from 1981 to 2016, the yearly temporal rainfall trend analysis of sixteen rain gauges was conducted. The findings showed that rainfall patterns vary significantly on yearly and seasonal basis, and that they are often unpredictable in character. The majority of the highland rainfall stations indicated declining trends on a yearly basis, according to the data. With the exception of Talagang station, the central and lowland stations in the research region observed an increasing trend of rainfall.

Asfaw et al. (2018) have used gridded monthly precipitation and temperature data from 1901 to 2014, trend analysis was used to examine the change in rainfall and temperature in northcentral Ethiopia. The coefficient of variation, precipitation concentration index, and Palmer drought severity index were used to analyze the data. The Mann-Kendall test was also used to detect a time series trend. The Mann-Kendall trend analysis test result revealed increasing trend for mean and minimum average temperatures through time significantly while the trend for maximum temperature exhibited a non-significant increasing trend. they recommend strategies designed in the agricultural sector have to take the declining and erratic nature of rainfall and increasing trend of temperature into consideration.

Kaur et al. (2021) have used the techniques of Mann Kendall test, and Sen's slope were used to analyse historical rainfall data on a monthly, annual, and seasonal basis for three locations in the lower Shivaliks of Punjab: Patiala-ki-Rao, Ballowal Saunkhri, and Saleran. The data trend analysis shows that the monthly rainfall is decreasing at Patiala-ki-Rao and Saleran.

The analysis of monthly, annual, and seasonal averages of rainfall and rainy days over a 15-year period revealed that both rainfall and rainy days decreased from 2001 to 2015 when compared to 1986 to 2000 during all seasons.

Gedefaw et al. (2018) carried out a research using the Mann-Kendall and Sen's slope estimator test to investigate the annual and seasonal rainfall variability at five selected stations in Amhara Regional State. The findings revealed that the annual rainfall trend in Gondar, Motta, and Bahir Dar stations was increasing. However, the trends in the Dangla and Adet stations were decreasing. In terms of monthly and seasonal variability of rainfall, all of the stations demonstrated change sensitivity. The findings of this paper may aid researchers in understanding the annual and seasonal variability of rainfall over the study region, as well as serve as a foundation for future research.

2.2 Regional Frequency Analysis

Nain & Hooda (2021) studied the region of Haryana, India with the 27 rain gauge stations to estimate maximum monthly rainfall quantiles using L-moments. Using Ward's cluster analysis method, these rain gauge stations were divided into three homogeneous regions. The L-moments ratio diagram and goodness-of-fit test were used to select a regional distribution for each homogeneous region. The results showed that the Generalized Logistic and Generalized Extreme Value distributions were the best-fitted regional frequency distributions for Regions 1 and 2, respectively, while Pearson Type-3 was the best-fitted distribution for Region 3. The quantiles for each region were determined, and regional growth curves were created. For the regional quantiles, the accuracy assessment was done using Monte Carlo simulations. The results of simulations revealed that uncertainty in regional quantiles, as measured by the Root Mean Square Error value and 90 percent error limits, was small when the return period was short, but increased as the return period lengthened.

Mesbahzadeh et al. (2019) investigated the frequency of floods in the Loot Basin, central Iran, using yearly peak discharge series and the maximum L-moment approach. The ZDIST statistic is used to choose a regional Log Pearson Type III (LPIII) distribution. The results also revealed a strong correlation coefficient between the return period and flood discharge, and the link between flood discharge and area parameters could be estimated. These strategies can be employed in regions where there is a dearth of observational data or statistics.

Hussain et al. (2017) have presented a study of Annual Maximum Monthly Rainfall Totals (AMMRT) regional frequency analysis of seven locations in Pakistan's Sindh. Preliminary testing has revealed that the data series are identically distributed, random, and lack any serial correlation. The three distributions; GNO, PE3 and GPA are acceptable candidates for regional distribution, according to the findings of the L-moment ratio diagram and ZDIST statistic. Study is helpful for agricultural water management, flood disaster prevention measures, and presented improvement projects for the reconstruction and modernization of important Indus River barrages in the Sindh Province.

Ali et al. (2017) have studied seasonal and yearly trends of rainfall for six meteorological stations in Gilgit Baltistan (GB) (a mountainous area of Pakistan) were studied in this study from 1980 to 2015. Mann-Kendall (MK) and Sen's slope (SS) nonparametric approaches were used to determine the intensity and size of trends at the 10% significance level. The Trend Free Pre-Whitening (TFPW) approach was used to reduce serial correlation in data. The results showed that mean annual precipitation was increasing at five sites (significant only at Gupis with an SS of 7.34 mm/year) and decreasing at one station (Astore) with an SS of -3.05 mm/year.

Ahmad et al. (2017) in their study used the index flood approach based on L-moments to estimate regional quantiles of Annual Total Rainfall (ATR) for 30 meteorological stations.

The study area was separated into four distinct areas. Using the L-moment ratio diagram and Z-statistic, the best fit distribution was identified. For the first three areas' big return periods, PE3 was judged to be the best option, while GNO and GEV were best for minor return periods. In a similar vein, area IV's GEV was determined to be the greatest fit for smaller return periods up to 20 years, while GNO was the best for periods of 50, 100, 500, and 1000 years.

Nair et al. (2014) have done research to better understand the regional rainfall variability and trend for this state during the past 100 years. In Kerala, it has been discovered that the rainfall varies greatly and on various timelines in the northern and southern areas. The mean and variability of rainfall change with the seasons. In most locations of Kerala, there is a considerable (99%) falling tendency in rainfall during the past 100 years, notably in the months of January, July, and November. In the majority of Kerala's areas, both annual and seasonal patterns in rainfall are shown to be substantially declining. This declining trend could be connected to climatic anomalies brought on by rising anthropogenic greenhouse gas (GHG) emissions from burning fossil fuels, changing land use owing to industrialization and deforestation, and a rise in air pollutants linked to traffic.

Ahmad et al. (2015) analyzed the L-moments (MLM), TL-moments (MTLM), and maximum likelihood estimate (MLE) approaches in order to identify the best-fit distribution of annual maximum stream flow (AMSF) data for at-site flood frequency analysis (FFA) in Pakistan,. Initially, this research looked at several probability distributions. Different goodness of fit tests, such as mean absolute deviation index (MADI), Anderson darling (AD) test, probability plot correlation coefficient (PPCC), and L-moments ratio diagram, are used to determine the best distribution for each site. We also projected different return durations associated with different flood magnitudes for on-site FFA. It is discovered that predicted flows based on fitted distributions agree closely with observed flows.

Yin et al. (2016) used regionalization approaches to improve knowledge of the regional frequency of severe precipitation. The data was initially checked for stationarity, serial dependency, and inter-site dependence. Through cluster and homogeneous analysis, the entire region was divided into four homogeneous regions. Generalized extreme-value (GEV) and generalized normal (GNO) distributions were selected as the best fitted distributions for most of the sub-regions using the goodness-of-fit statistic and L-moment ratio diagrams. Monte Carlo simulation was performed to assess the accuracy of the quantile estimations while accounting for inter-site dependency.

Reiter et al. (2012) carried out a study at temperature and precipitation trends in instrumental time series from 1960 to 2006 at 88 Upper Danube Basin meteorological stations. The findings support a particularly substantial recent Climate Change in the study region. In the summer, increasing temperature trends exhibit exceptionally high trend values of up to 0.8°C/decade. The findings support a particularly substantial recent Climate Change in the study region. In the summer, increasing temperature trends exhibit exceptionally high trend values of up to 0.8°C/decade.

Hansen (2015) has applied regional frequency analysis L-moments approach at 12 rain gauge sites in southern Alberta for rainfall durations ranging from 1 hour to 24 hours in this study. The best-fit regional frequency distribution was used to estimate rainfall quantiles for return periods up to 1:1000 years. The quantiles were compared to the quantiles obtained using the traditional on-site Gumbel approach. The results revealed that the conventional approach tends to underestimate the quantiles in comparison to the regional approach, particularly for sub-daily rainfall durations. For the 1:100-year return period, the accuracy of the two approaches was tested using Monte Carlo simulations, and the results showed that the root mean square error (RMSE) using the conventional approach is approximately 2-2.5 times greater than the error using the regional approach. Regional frequency analysis has yet to reap

its full benefits in Canada, which could benefit from a national program to update rainfall IDF estimates using these more statistically robust approaches.

Khan et al. (2017) carried out research on regional frequency analysis of extreme precipitation based on monthly precipitation records (1999–2012) from 17 stations in Pakistan's Northern Areas and Khyber Pakhtunkhwa based on L-moments and partial L-moments. For generalized extreme value (GEV), generalized logistic (GLO), generalized normal (GNO), and generalized Pareto (GPA) distributions, the L- and PL-moments are derived. The statistical characteristics of extreme precipitation in GB and Khyber Pakhtunkhwa, Pakistan, were identified as being represented by the Z-statistics and L- and PL-moments ratio diagrams of the GNO, GEV, and GPA distributions. In order to investigate the sampling characteristics of L- and PL-moments, Monte Carlo simulation was used. The findings demonstrate that PL-moments outperform L-moments for estimating major return period events.

Asong et al. (2015) have applied a new approach to identify homogeneous regions for regionalization of precipitation characteristics for the Canadian Prairie Provinces. According to the findings of the analyses, the study area can be divided into five homogeneous regions. These partitions are validated for homogeneity independently using statistics computed from monthly and seasonal precipitation totals, as well as seasonal extremes from a network of observation stations. Furthermore, precipitation magnitude-frequency relationships of warm and cold season single- and multi-day precipitation extremes developed through regional frequency analysis are spatially mapped based on the identified regions. Such estimates are critical for a variety of water resource-related activities.

Chapter 3

MATERIALS AND METHODS

3.1 Study Area

The area under consideration is Gilgit Baltistan. The spatial extent of Gilgit Baltistan is 34^{o} 32' 24" N to 37^{o} N Latitude and 72^{o}32' 24" E to 78^{o} E Longitude, covers 72,971 square kilometres, approximately half of which is covered by mountain peaks, glaciers, lakes, and highlands. There are 14 mountain summits exceeding 8,000 meters in the globe, five of which are situated in the Gilgit Baltistan. At least 5,000 large and minor glaciers, including some of the world's longest outside the polar zone are in this area, makes mainland populations to rely significantly on mountain water for household, agricultural, energy, and industrial needs.

Being the northern and mountainous region of the country, Gilgit Baltistan has long with high precipitation winters and short and wet summers. The climate is continental, with a considerable temperature fluctuation between winter and summer. From December to May, the northern areas are more prone to cold fronts produced by the westerly winds of the middle latitudes, as well as being the coldest at similar height. The annual rainfall in Gilgit Baltistan is 860 mm and rainy seasons are winters and pre-monsoon. However, not all regions receive a lot of rain; it all depends on the slope exposure. The southern side (the mountains north of Peshawar and Islamabad) receives significantly more rainfall than the northern. The location map is shown in fig. 1.

The monthly dataset of precipitation for 15 stations in Gilgit Baltistan is obtained from Pakistan Meteorological Department. The location of study area is shown in fig 1. However, the data for some stations are of limited time period. Furthermore, any kind of inconsistencies or missing data was replaced by average value of same month from previous and later year.

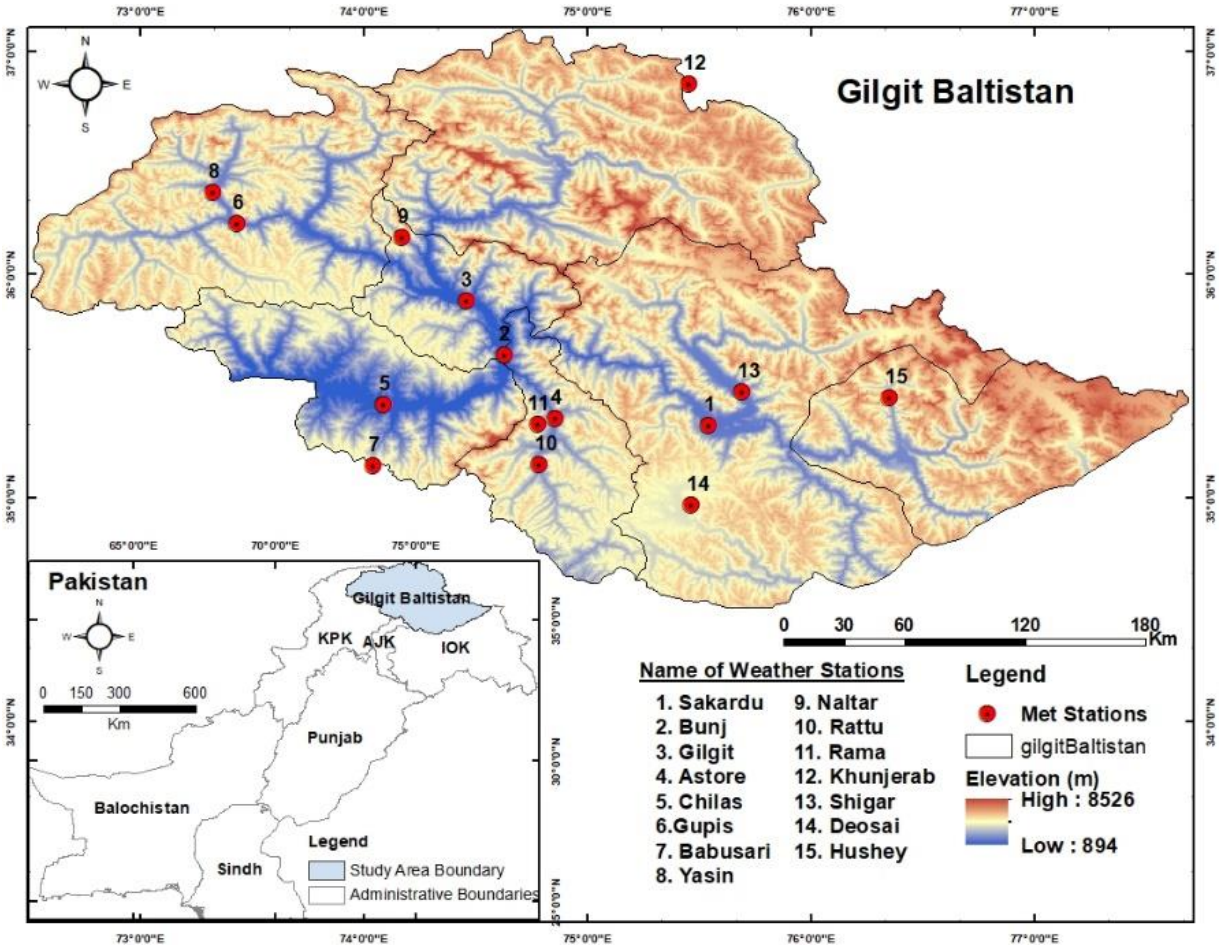

Fig. 2.1 Location map of Gilgit Baltistan.

Table 2. 1 Characteristics of fifteen sites in Gilgit Baltistan, Pakistan.

Sr. No.	Rain Gauge Stations	Latitude (North)	Longitude (East)	Altitude	Data Range
1.	Sakardu	35.3247	75.551	2227 m	1990 - 2020
2.	Bunji	35.6431	74.6342	1452 m	1990 - 2020
3.	Gilgit	35.8819	74.4643	1442 m	1990 - 2020
4.	Astore	35.357	74.8624	2372 m	1990 - 2020
5.	Chilas	35.4222	74.0946	1165 m	1990 - 2020
6.	Gupis	36.2274	73.4421	2205 m	1990 - 2020
7.	Babusar	35.1462	74.0482	4155 m	2006 - 2020
8.	Yasin	36.3694	73.3326	2369 m	1998 - 2019
9.	Naltar	36.1654	74.1786	2890 m	1998 - 2019
10.	Rattu	35.1523	74.7934	2684 m	1998 - 2019
11.	Rama	35.3304	74.7856	3474 m	1998 - 2019
12.	Khunjerab	36.8539	75.4589	4678 m	1998 - 2019
13.	Shigar	35.4765	75.6964	2287 m	1998 - 2019
14.	Deosai	34.9705	75.4718	4206 m	1998 - 2019
15.	Hushey	35.4504	76.3585	3160 m	1998 - 2019

3.2 General Methodological Design

In this study the statistical trend analysis of precipitation from 1990 to 2020 is done by using the techniques of Mann Kendal and Sen's Slope Estimate. Mann Kendal test is a non-parametric hypothesis test that is used to detect the presence of statistically significant trend. In this test null hypothesis assumes that trend is present in time series whereas alternative hypothesis denies the presence of any kind of trend in dataset. Sen's Slope further, estimates the magnitude of slope this trend in data series.

Along with the quantitative study to measure the changing trends and variability in precipitation, the estimation of magnitude and frequency of precipitation events is done, for it is of utmost importance as extreme precipitation events are one of the most disastrous hydrometeorological events. For that purpose, frequency analysis is done, frequency analysis is the estimation of how frequently a specified event will take place. There are several conventional techniques for regional frequency analysis but there are many uncertainties in estimation of frequencies of precipitation events. The accurate estimation is important in building hydraulic structure like spillways, dikes, storm surge barriers and dams. Several statistical and probabilistic techniques are used in their estimation. Among different methods of regional frequency analysis, the regional index flood type approach based on L-moments has many reported benefits. The basic procedure of frequency analysis includes identification of homogenous regions, testing of frequency distribution, estimation of parameters and quantiles at stations of interest.

The general methodological flowchart is shown in fig. 3 and the datasets which has been used in this study with their sources are given in the table.

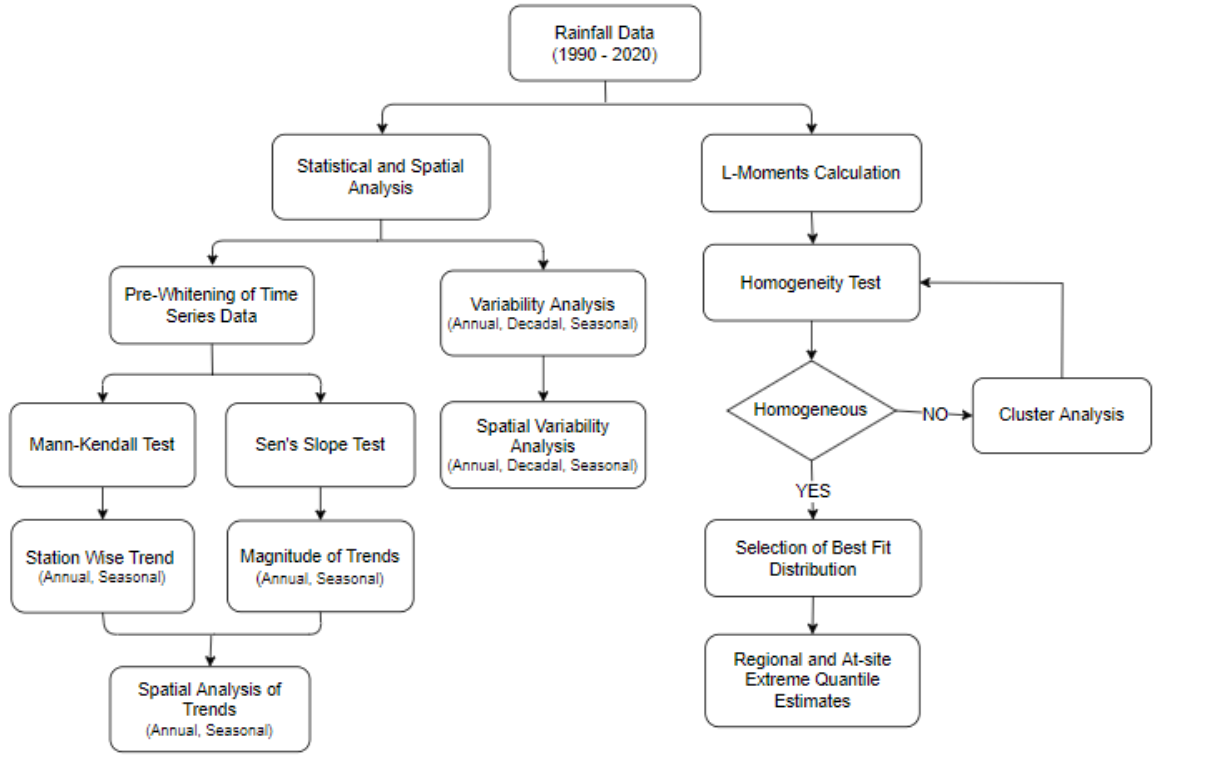

Fig. 2.2 General methodological flowchart.

Table 2. 2 Datasets description and sources.

Data	Description	Source
Precipitation Data	Precipitation data of 15 stations in Gilgit Baltistan from 1990 to 2020	Pakistan Meteorological Department
DEM	**Aster**	USGS earth explorer https://earthexplorer.usgs.gov
Software Used		
ArcGIS (10.8)	Geospatial analysis	ESRI and University of Chicago
Microsoft Excel	Data Trend Analysis	Microsoft

3.3 Mann Kendall Trends Test

Mann Kendall test is a nonparametric test for the detection of statistical trend in data series. The MK test requires serially independent time series data or it gives wrong indication of trend. The presence of autocorrelation would boost the chance of a significant trend to the data series, affecting the MK test results. Hence the Pre-whitening of data series is preferred by calculating lag-1 serial correlation coefficient (r_1) for each time series.

$$\mathbf{r_1 = \frac{1/n-1 \ \sum_{i=1}^{n-1}(x_i - \bar{x})(x_{i+1} - \bar{x})}{1/n \ \sum_{i=1}^{n-1}(x_i - \bar{x})^2}} \quad \textbf{3.1}$$

where $\bar{x}$ is mean of time series.

If the condition ((-1-1.645√(n-2) /(n-2)) ≤ r_1 ≤ ((-1+1.645√(n-2) /(n-2)) is satisfied the data is independent of autocorrelation at 10% significance level. If the condition is not satisfied, then the autocorrelation is removed by

$\mathbf{x_2 - r_1 x_1,\ x_3 - r_1 x_2, \dots, x_n - r_1 x_{n-1}}$ ..

Mann Kendall test checks the null hypothesis for no trend and an alternative hypothesis for the presence of trend, that could be increasing or decreasing monotonically. The MK test is defined as:

$$\boldsymbol{S = \sum_{i=1}^{n-1} \sum_{j=i+1}^{n} sgn(x_j - x_i)} \quad \textbf{3.2}$$

Where x_j and x_i are sequential data series. $sgn(x_j - x_i)$ is calculated as follows:

$$\boldsymbol{sgn(x_j - x_i) = \begin{cases} 1, & if\ x_j - x_i > 0 \\ 0, & if\ x_j - x_i = 0 \\ -1, & if\ x_j - x_i < 0 \end{cases}} \quad \textbf{3.3}$$

positive and negative values of S represent increasing and decreasing trend respectively. If there are 10 or more data values, the S statistic approximates normal distribution, and the test is run with a normal distribution with the mean and variation as shown below:

$$E(S) = 0 \tag{3.4}$$

$$V(S) = \frac{n(n-1)(2n+5) - \sum_{i=1}^{m} t_i(t_i-1)(2t_i+5)}{18} \tag{3.5}$$

Where m is total number of tie groups in data and t_i is the number of data points in the ith tie group.

Statistically significant trend is identified by Z score, that is calculated as follows:

$$Z = \begin{cases} \frac{S-1}{\sqrt{Var(S)}} & if\ S > 0 \\ 0, & if\ S = 0 \\ \frac{S+1}{\sqrt{Var(S)}} & if\ S < 0 \end{cases} \tag{3.6}$$

positive score indicates a growing trend, whereas a negative value suggests a decreasing trend. With a null hypothesis of no trend, Z-statistics follow the normal distribution with an average of zero and a variance of one. Generally, α = 0.1 (10%) significance level with Z = ±1.645 is considered globally (Kaur et al., 2021).

3.4 Sen's Slope Method

Sen's slope technique is a nonparametric test that is used to forecast the magnitude of hydrometeorological time series data. Sen's slope estimator approach analyzes trends using a linear model. The following equation is used to determine Sen's slope (T_i) for all data pairings.

$$T_i = \frac{x_j - x_k}{j-k} \quad \text{for } i = 1,2,3,\ldots,n \tag{3.7}$$

Where x_j and x_k are data values at times j and k (j > k). Sen's slope is estimated by taking median of all T_i values.

$$Q_i = \begin{cases} T_{(n+1)/2}, & if\ n\ is\ odd \\ \frac{1}{2}(T_{n/2} + T_{(n+2)/2}) & if\ n\ is\ even \end{cases} \quad 3.8$$

Sen's slope estimates depend upon the value of n, which can be odd or even, and (Q_{med}) is derived using a 100(1-α) percent confidence interval based on a normal distribution. A positive Qi number implies an increasing (upward) trend, whereas a negative Qi value denotes a declining (downward) trend in time series data (Gedefaw et al., 2018).

3.5 L-Moments

L-moments were suggested by J. R. M. Hosking (1990) as a substitute for standard statistical moments and as special cases of Probability Weighted Moments (PWM), which have better statistical properties in general. For example, they are robust to data outliers and allow for a more precise identification of the parent distribution that generated a particular sample of data.

For estimating the parameters of a probability distribution, the conventional moments technique can be utilized but conventional techniques, however, has several severe limitations. Wallis et al. [26] show that the ratio of moment estimators is biased and that the assumption of being normally distributed is frequently broken. Pearson (1991) adds that it is susceptible to outliers. As a result, it is not trustworthy for skewed distributions.

Probability weighted moments are defined as:

$$\beta_r = E[x\{F(x)\}^r] \quad 3.9$$

L-moments can be estimated through linear combinations of PWMs. The rth L-moment λ_r is related to the rth PWM through:

$$\boldsymbol{\lambda_{r+1}} = \sum_{\mathbf{k=0}}^{\mathbf{r}} \boldsymbol{\beta_r}(-\mathbf{1})^{\mathbf{r-k}} \binom{\mathbf{r}}{\mathbf{k}} \binom{\mathbf{r+k}}{\mathbf{k}} \qquad 3.10$$

Hosking (1990) defined L-moment ratios as:

L-CV: $\tau = \frac{\lambda_2}{\lambda_1}$

L-skewness: $\tau_3 = \frac{\lambda_3}{\lambda_2}$

L-kurtosis: $\tau_4 = \frac{\lambda_5}{\lambda_2}$

Analogous to which Hosking (1990) defined sample L-moments denoted by l_1, l_2, l_3, l_4 and sample L-moments ratios denoted by *t*, t_3 and t_4 (Hosking and Wallis, 1997).

3.6 Regional Frequency Analysis

The regional analysis methodology is based on L-moments proposed by Hosking and Wallis (1997). If we have data from large enough number of sites and quantile estimations are needed at each location, regional frequency analysis employing an index flood approach will entail these four steps.

- Initial Screening of Data
- Heterogeneity Measure
- Choice of the suitable probability distribution
- Estimation of regional quantiles

The initial stage of regional frequency analysis, like with any statistical study, is a detailed examination of data. Any discrepancies should be eliminated, and the data should be checked to ensure for its randomness, serial correlation and identical distribution. Several statistical tests

are performed which include Run test, lag-1 correlation coefficient and Mann Whitney test to check the randomness, serial correlation and identical distribution of all timeseries.

After the initial screening, data is checked for any discordant site, that simply means of any inconsistency in data of any site. The whole region under consideration is subjected to homogeneity test, which implies that all the locations in a homogenous region are assumed to have identical frequency distribution. If the criteria are not satisfied, with the help of cluster analysis the region is divided into small more than one homogenous regions. Then most suitable probability distribution is tested for all homogenous regions with the help of two techniques, L-moments ratio diagram and Z^{DIST} criteria. The regional and at-site quantiles are calculated with the help of the selected probability distribution.

3.6.1 Initial Screening of Data

Regional frequency analysis is based on specific assumptions about the observed data series, namely that the data series at the given site(s) is random, not serially correlated, and is distributed similarly. As a result, multiple statistical tests were used to perform a preliminary screening of the observed data set. The randomness of the data series at specific locations was assessed using a non-parametric test, namely the Run-test. The Lag-1 correlation coefficient (r1) was used to test for the presence of serial correlation in the data series at specific locations. The Mann-Whitney Test was used to test the hypothesis that the sample (data series at a particular location) is uniformly distributed.

3.6.2 Discordancy Measure

A discordancy measure (Di) based on L-moments was utilized to look for any discordant sites in an area. The Di for site i in a collection of N sites is

$$D_i = \frac{1}{3} N(u_i - \bar{u})^T A^{-1} (u_i - \bar{u}),\ i = 1,2,\dots,N$$

$$A = \sum_{i=1}^{N} (u_i - \bar{u})\,(u_i - \bar{u})^T$$

$$u_i = [t^{(i)}\ t_3^{(i)}\ t_4^{(i)}]^T$$

$$\bar{u} = N^{-1} \sum_{i=1}^{N} u_i$$

During data screening, N denotes the number of stations in the region, and the statistic D i was determined for each station (Ahmad et al., 2017). The acceptable range for this dataset, for a site to be not discordant is less than 3.

3.6.3 Heterogeneity Measure

Heterogeneity measure determines the degree of heterogeneity in a group of sites i.e., the homogeneity criterion states that the frequency distributions of the locations are identical in a homogeneous region. Hosking and Wallis (1997) suggested heterogeneity measure (H) based on the standard deviation (V) of the at-site sample L-CVs weighted proportionally to the site's record duration. Heterogeneity measure is calculated as

$$\mathbf{H} = \frac{\mathbf{V} - \boldsymbol{\mu}_\mathbf{v}}{\boldsymbol{\sigma}_\mathbf{v}} \qquad 3.11$$

Where μ_v is σ_v are mean and standard deviation of the values of V obtained from simulations. A region is

homogeneous if H < 1,

possibly heterogeneous if $1 \leq H < 2$,

heterogenous if $H \geq 2$.

3.7 Selection of the Suitable Probability Distribution

3.7.1 L-moment Ratio Diagram

L-moment ratio diagram is a plot between L-skewness and L-kurtosis that helps select the appropriate frequency distribution. The sample weighted average's closeness to a specific candidate distribution theoretical curve or point in (L-Cs, L-Ck) space has been regarded as an indicator of that distribution's suitability to characterize regional data. Regional growth curves are constructed for a homogenous region, and it is assumed that all stations in that region have same frequency distribution.

3.7.2 Z^{DIST} Criteria

Another criterion for choosing the best-fit distribution is the Z statistic DIST, which was developed by Hosking and Wallis (1993) with the goal of comparing simulated L-Cs and L-Ck of a fitted distribution with regional average L-Cs and L-Ck values derived from actual data. It is measured as

$$Z^{DIST} = \frac{\tau_4^{DIST} - t_4^R + B_4}{\sigma_4} \qquad 3.12$$

Where τ_4^{DIST} is the L-kurtosos of the fitted Kappa distribution, t_4^R is L-kurtosis, B_4 is the bias of t_4^R, and σ_4 is the simulated standard deviation of t_4^R.

A suitable match for a given distribution is the one with the $|Z^{DIST}| \leq 1.64$. This quality of fit criterion may be qualified by a number of distributions. Then the most appropriate distribution will then be the one with the lowest $|Z^{DIST}|$ value.

3.8 Regional Rainfall Quantile Estimation

The index rainfall approach is used to estimate quantiles for different probability levels or return periods after the proper frequency distribution for each homogeneous region has been found. Except for the site-specific scale parameter or an index factor, the approach assumes that maximum daily rainfall data at multiple locations in a homogenous region have the same distribution. The scale factor is designated as an index-rainfall and is commonly assumed to represent the yearly maximum daily rainfall. The quantile estimates Q(F), with non-exceedance probability F at a site in a region with N sites are computed as $\boldsymbol{Q_i(F) = l_1 \hat{q}(F)}$ where q is a common dimensionless quantile function (regional growth curve) and l_1 is the index rainfall value, representing the T-year quantile of the normalized regional distribution.

At-site quantiles are estimated by multiplication of site specific average annual maximum rainfall with the calculated regional quantiles to generate the appropriate rainfall quantiles for the relevant station using the regional parameters for the similar distribution at different return periods. Moreover, stations with historic extreme events and are identified as higher risk stations for floods and other related meteorological disasters. Vulnerability of sites are assessed by corresponding historic flood events at specific sites and the extreme rainfall quantile estimates for such regions are useful for disaster prevention planning and disaster mitigation plannings (Ahmad et al., 2017).

Chapter 4

RESULTS AND DISCUSSION

4.1 Statistical Trends

In this study, rainfall trend analysis is carried out for fifteen stations in Gilgit Baltistan for past three decades using Mann Kendall trend test and Sen's Slope. $P < 0.05$ shows the presence of statistically significant trend in time series whereas positive and negative values of Q score represent the magnitude of increasing and decreasing trends in rainfall.

The results of statistical trend test have shown that three stations namely Astore, Khunjerab and Hushey have significant annual trends whereas, four stations namely Astore, Khunjerab, Babusar and Yasin have shown seasonal trends in different seasons. All rest of the stations do not have any statistically significant trend of rainfall present in their dataset. The results are shown in table 3 in which Q score is the magnitude of trend.

Fig. 3.1, 3.2 and 3.3 show the annual rainfall trends in Hushey, Khunjerab and Astore. Hushey has experienced an increase in rainfall of about 11.47 mm per year. Khunjerab station shows an increasing annual rainfall trend of 10.47 mm per year and the rainfall in Astore is decreased by 6 mm per year. Hence Astore is the only station in Gilgit Baltistan where rainfall has been decreased over past three decades.

Fig. 3.4 and 3.5 show the rainfall trends of Babusar station in its monsoon and winter seasons respectively. Monsoon rainfall is increasing by 1.8 mm per year and winters rainfall is decreasing by 2.76 mm per year. Fig. 3.6, 3.7 and 3.8 show seasonal rainfall trends of Astore, Yasin and Khunjerab respectively. In Astore pre-monsoon rainfall is decreasing by 1 mm per year whereas in Yasin the season of post-monsoon shows increasing trend of 0.45 mm and in Khunjerab monsoon season shows an increase in rainfall of 0.55 mm per year.

Table 3. 1 Statistical trends of rainfall in Gilgit Baltistan.

Time Series	Astore		Khunjerab		Hushey		Babusar		Yasin	
	P value	**Q score**	**P value**	**Q score**	**P value**	**Q score**	**P value**	**Q score**	**P value**	**Q score**
Monsoon (JJAS)	0.70	-0.11	**0.01**	**0.55**	0.09	0.51	**0.03**	**1.79**	0.11	-0.57
Post-monsoon (ON)	0.94	-0.03	0.08	0.57	0.15	0.27	0.65	0.07	**0.02**	**0.45**
Winter (DJF)	0.08	-0.87	0.09	1.12	0.65	0.35	**0.03**	**-2.76**	0.57	0.34
Pre-monsoon (MAM)	**0.04**	**-0.95**	0.14	0.66	0.31	0.49	0.96	-0.03	0.39	-0.69
Annual (J-D)	**0.03**	**-6.04**	**0.00**	**10.47**	**0.02**	**11.47**	0.19	-0.61	0.86	-0.09

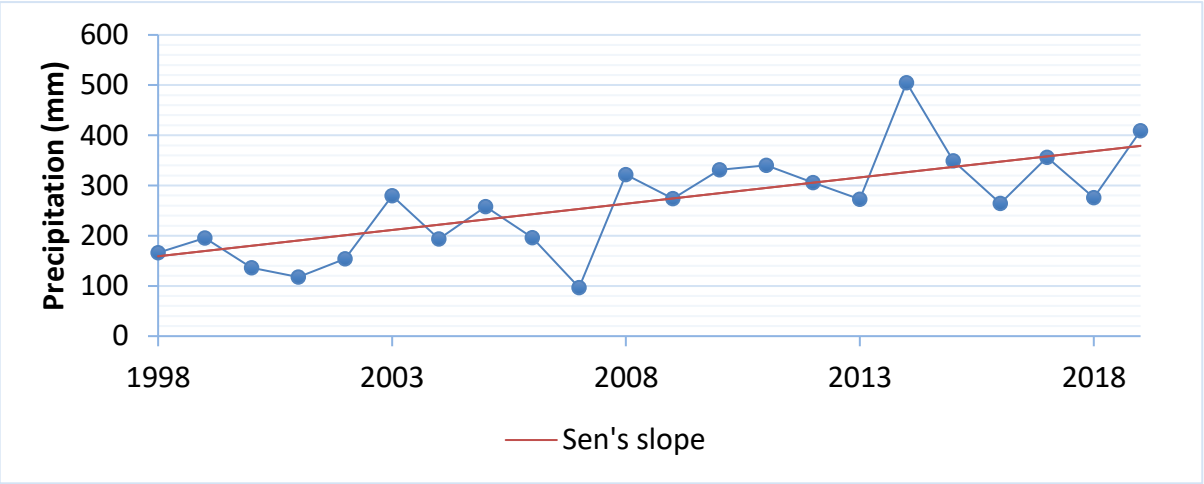

Fig. 3.1 Khunjerab annual rainfall trends.

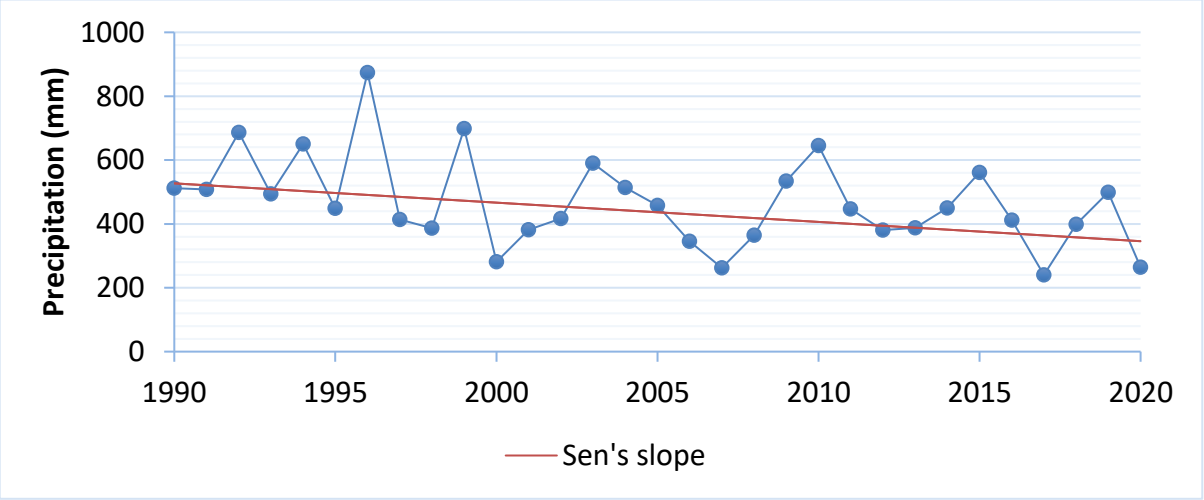

Fig. 3.2 Astore annual rainfall trends.

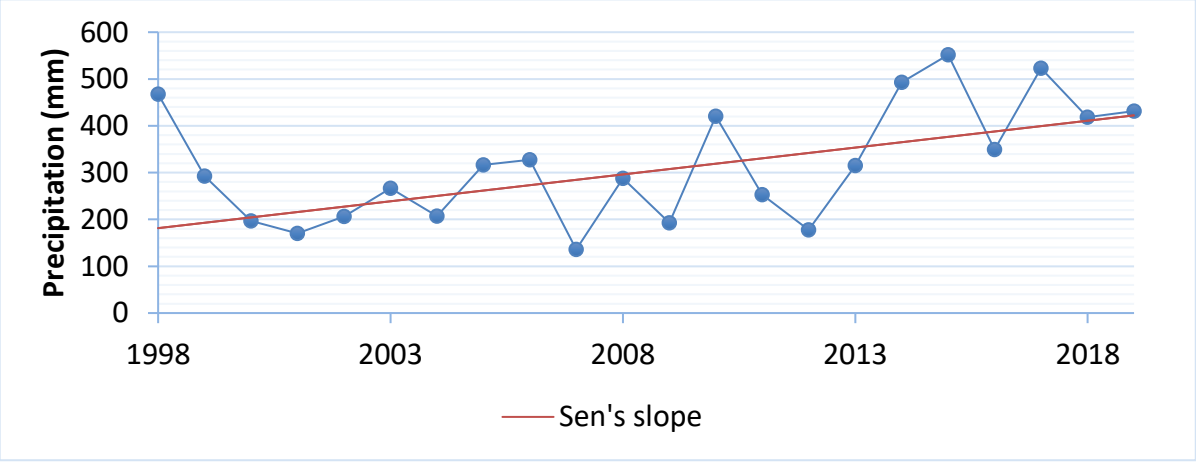

Fig. 3.3 Hushey annual rainfall trends.

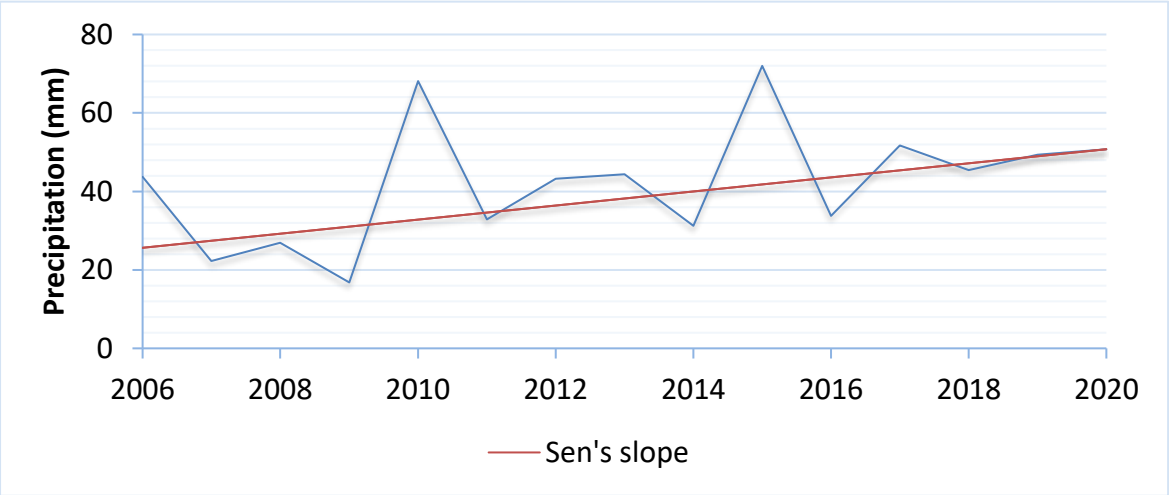

Fig. 3.4 Babusar monsoon rainfall trends.

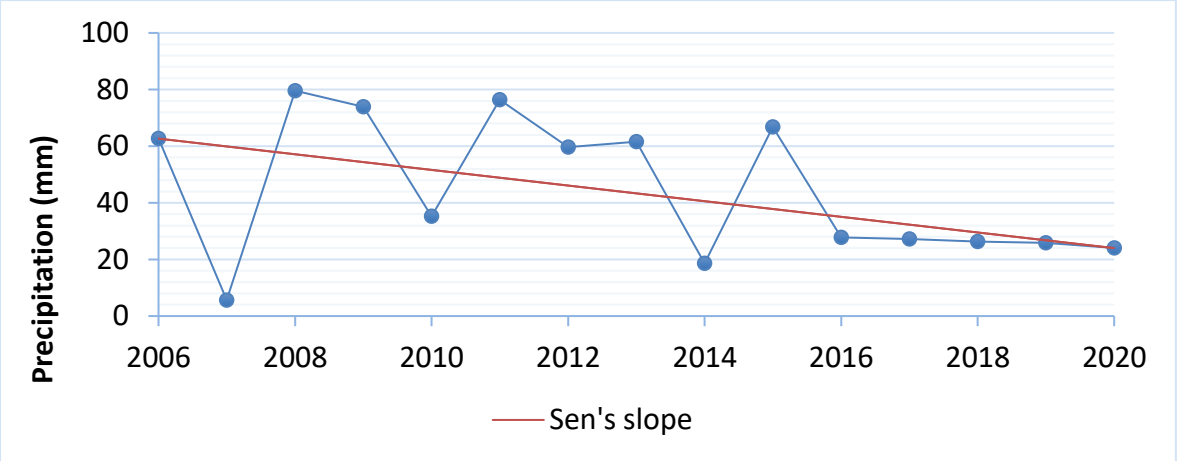

Fig. 3.5 Babusar winters rainfall trends.

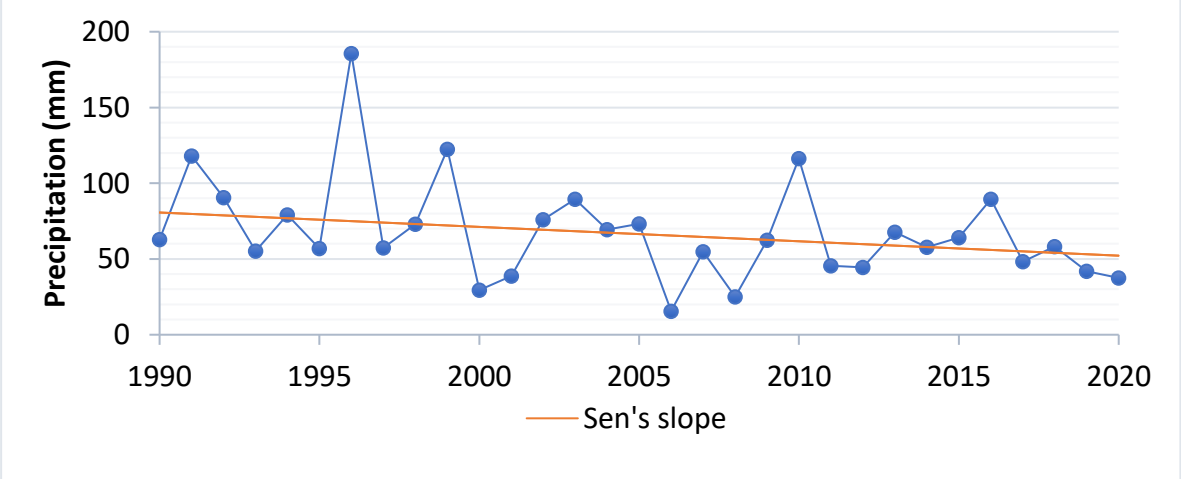

Fig. 3.6 Astore pre-monsoon rainfall trends.

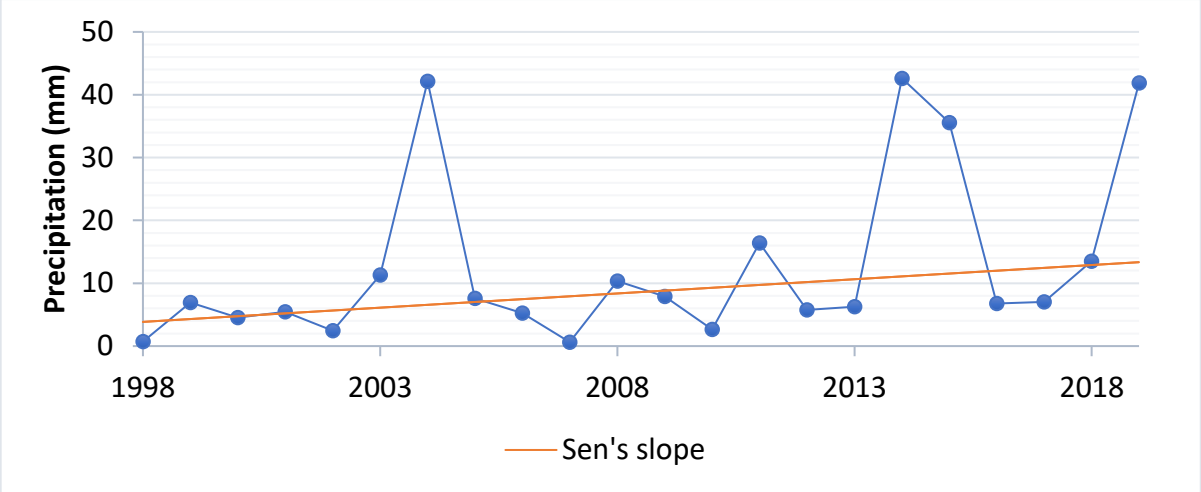

Fig. 3.7 Yasin post-monsoon rainfall trends.

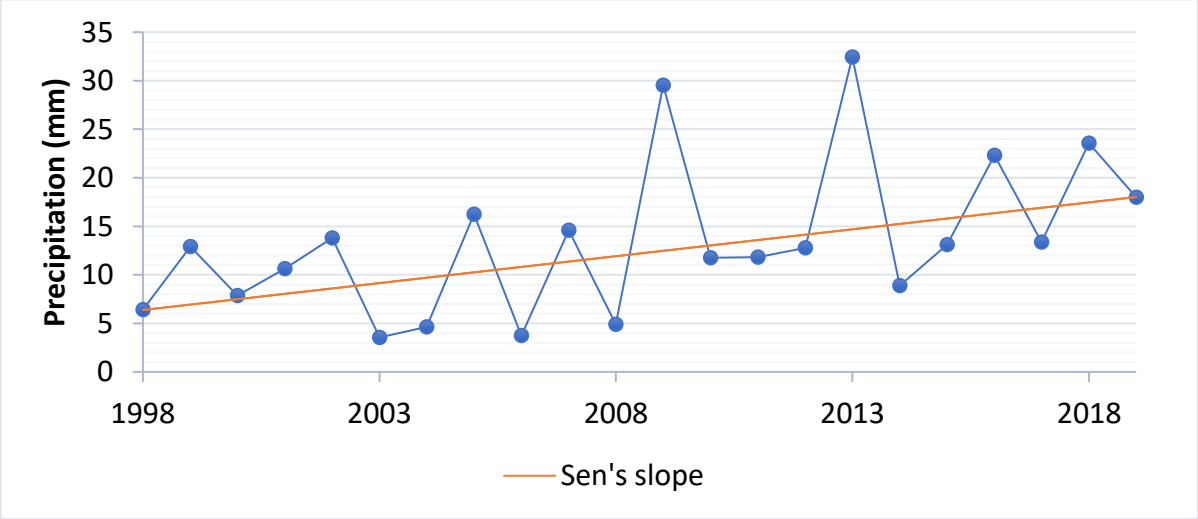

Fig. 3.8 Khunjerab monsoon rainfall trends.

4.2 Spatial Trends

The annual and seasonal spatial rainfall trends analysis is done using inverse weightage distance technique of interpolation. Figure 3.9 shows the annual rainfall trends of three decades from 1990 to 2020. According to the Pakistan Meteorological Department's categorization, the seasons are divided into four groups: Winter (January, February and December), Pre-monsoon (March, April, May), Monsoon (June, July, August, September), and Post-monsoon (October and November). The spatial distribution shows there is great variation in rainfall trends on annual basis i.e., from decreasing trends of magnitude 8 mm per year to increasing trend of 11.5 mm per year, all over Gilgit Baltistan. Rainfall trends are increasing in North and Northeast parts and decreasing in South and Southwest parts of GB. The district of Hunza Nagar and Ghanche have experienced increasing rainfall trends, whereas districts of Ghizer and Diamer have experienced decreasing rainfall trends. Moreover, some regions in Sakardu and Astore districts also showed slightly decreasing trends.

Fig. 3.10 shows seasonal rainfall trends in Gilgit Baltistan. Although most of the rainfall occurs in Pre-monsoon and Winters season in GB, decreasing trends in rainfall are observed in Winters and Pre-monsoon seasons. The decreasing trends are observed in Southern areas of Gilgit Baltistan i.e., lower regions of Diamer and Sakardu district. Rainfall trends are increasing in Hunza Nagar and Ghanche districts in Winters and Pre-monsoon. The season of Monsoon also showed slightly increasing trends in Eastern regions of Gilgit Baltistan. The season of Post-monsoon showed insignificant trends in rainfall.

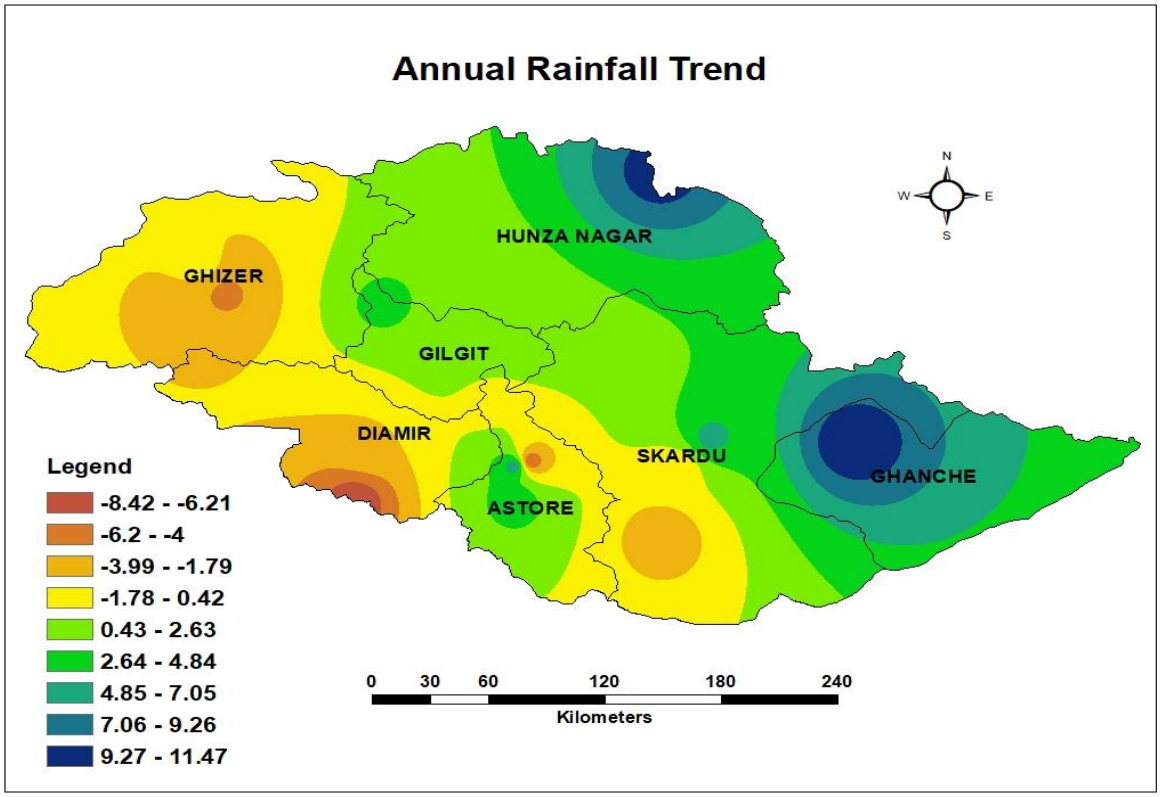

Fig. 3.9 Annual rainfall trends of Gilgit Baltistan.

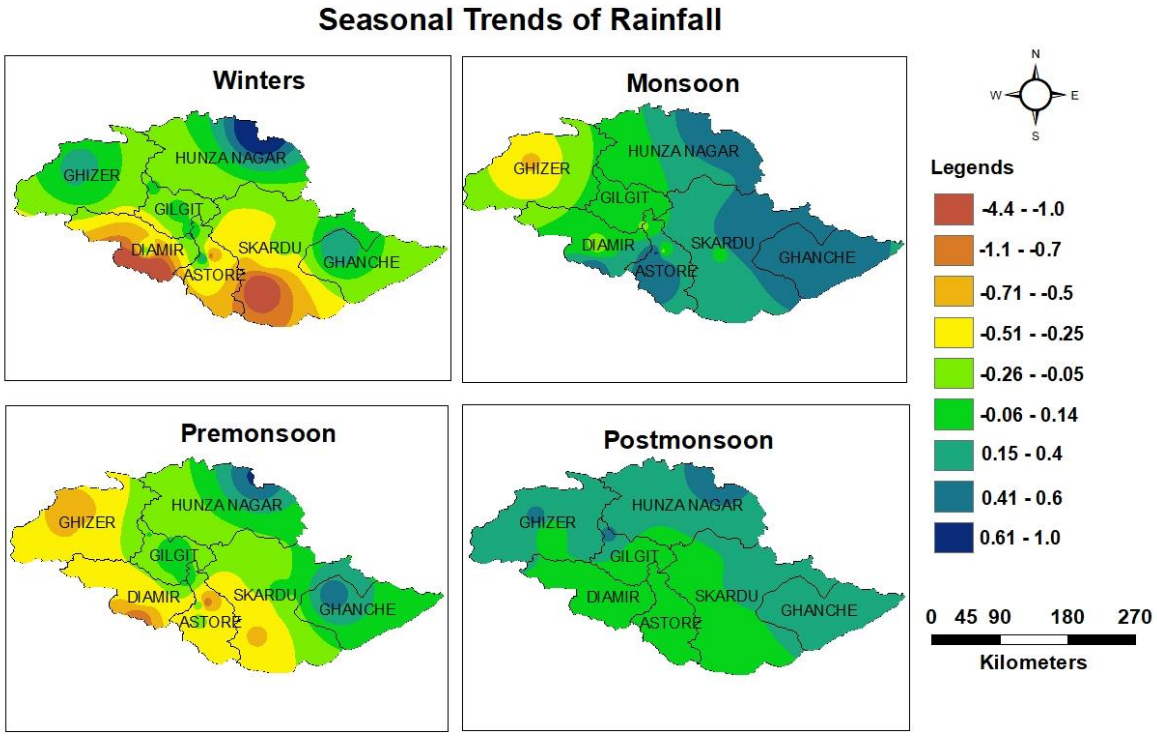

Fig. 3.10 Seasonal trends of rainfall in Gilgit Baltistan.

Rainfall variability in Gilgit Baltistan for over three decades using coefficient of variation on annual, seasonal and decadal basis. Fig. 3.11 shows rainfall variability on annual basis. Rainfall of Astore district is less variable i.e., ranges from 23 to 35% variability in average rainfall as compared to rest of the province as Astore receives highest rainfall. Whereas rainfall of district of Ghizer has highest variability i.e., ranges from 35 to 60% variability in average rainfall as Ghizer receives lowest rainfall. Districts of Hunza Nagar, Gilgit and Sakardu showed rainfall variability from 27 to 40%. Ghanche district has rainfall variability ranges from 36 to 40% whereas the district of Diamer observed rainfall variability ranges from 36 to 50%.

Fig. 3.12 shows seasonal rainfall variability in Gilgit Baltistan. In rainy season, variability of rainfall is highest Ghizer district ranges from 66 to 164%. And lowest in southern regions of Sakardu and Astore districts. The pre-monsoonal rainfall variability is highest in Ghizer district ranges from 66 to 100% and lowest in eastern regions including Ghanche, Sakardu and Hunza Nagar districts. In monsoonal rainfall, low variability is recorded for almost all over GB. However, relatively high rainfall variability is recorded in some areas of Ghanche district.

Moreover, from 1990 to 2000 highest rainfall variability is recorded in some areas of districts of Diamer, Ghizer and Gilgit ranges from 28 to 62%. And relatively lower variability is recorded on eastern regions of Gilgit Baltistan. From 2001 to 2010, highest variability is observed in the districts of Hunza Nagar and Ghizer. However, other regions of province observed moderate rainfall variability. In the decade of 2011 to 2020, highest variability was observed in the areas of Diamer and Hunza whereas, lowest variability was observed in the districts of Ghizer and Gilgit ranges from 14 to 27%. Rest of the districts of Sakardu, Astore and Ghanche observed moderate rainfall variability ranges from 28 to 41%. Fig. 3.13 shows decadal variability of rainfall.

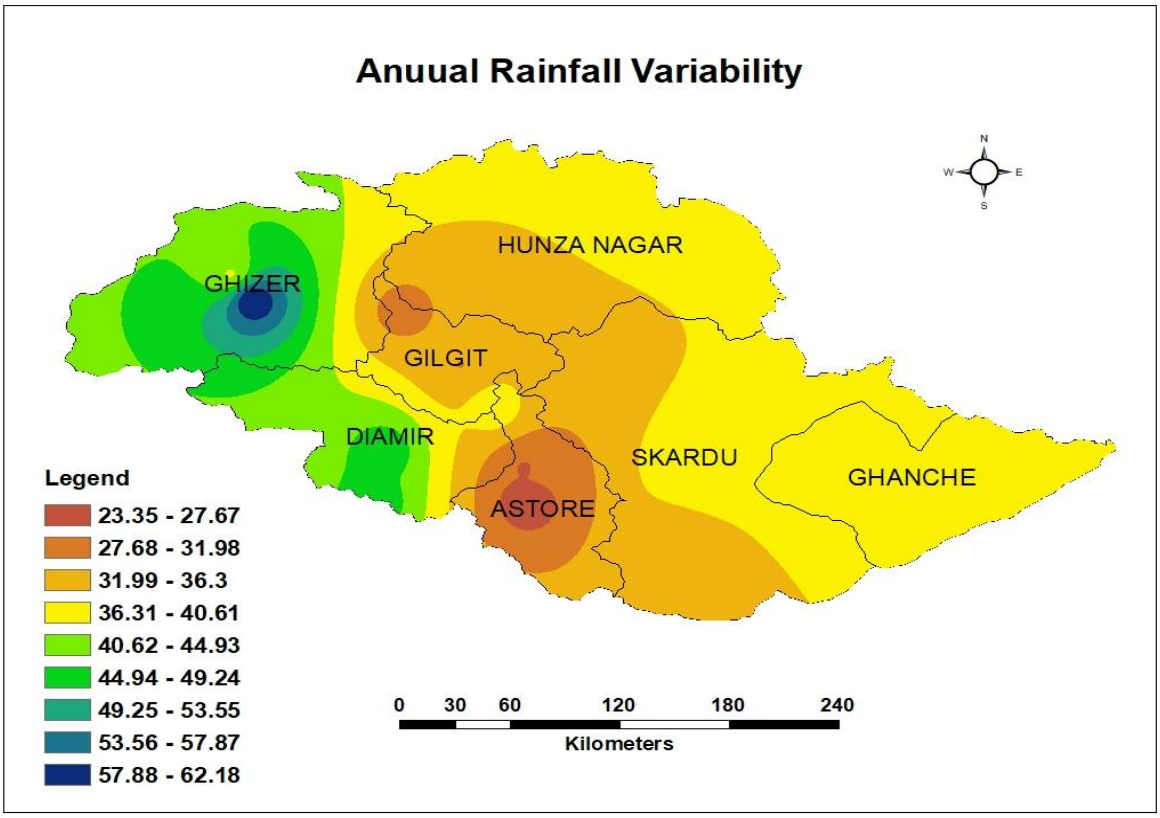

Fig. 3.11 Annual rainfall variability in Gilgit Baltistan.

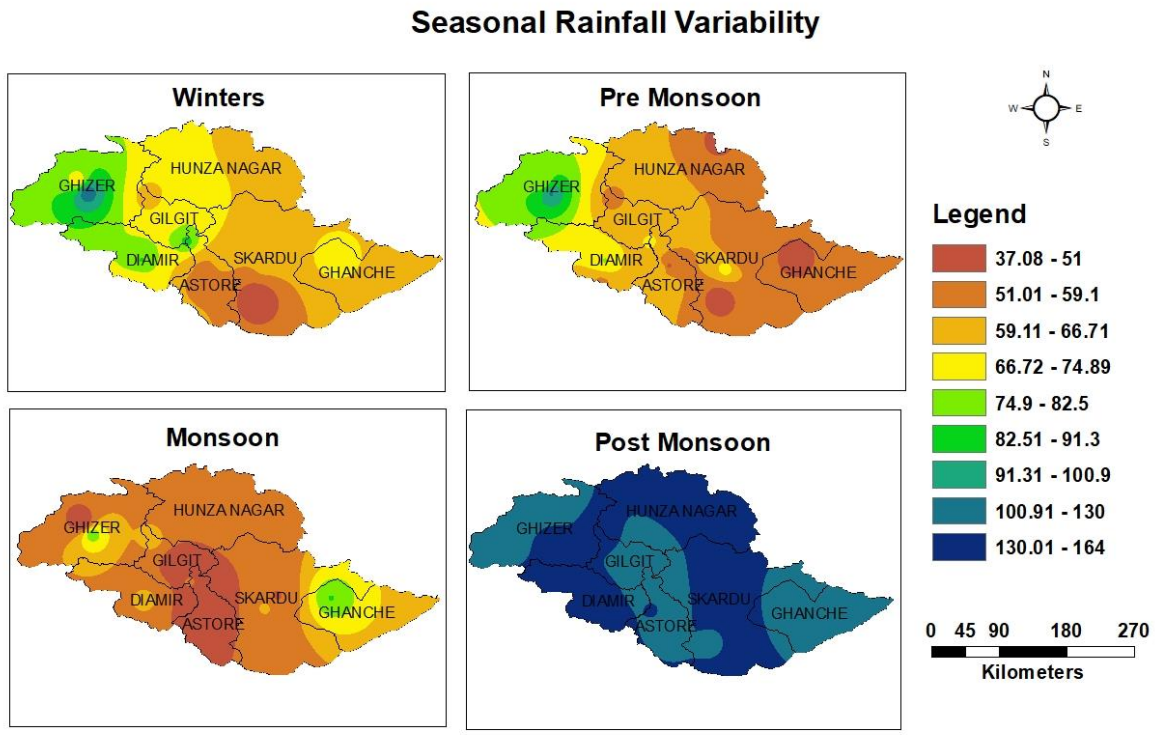

Fig. 3.12 Seasonal rainfall variability in Gilgit Baltistan.

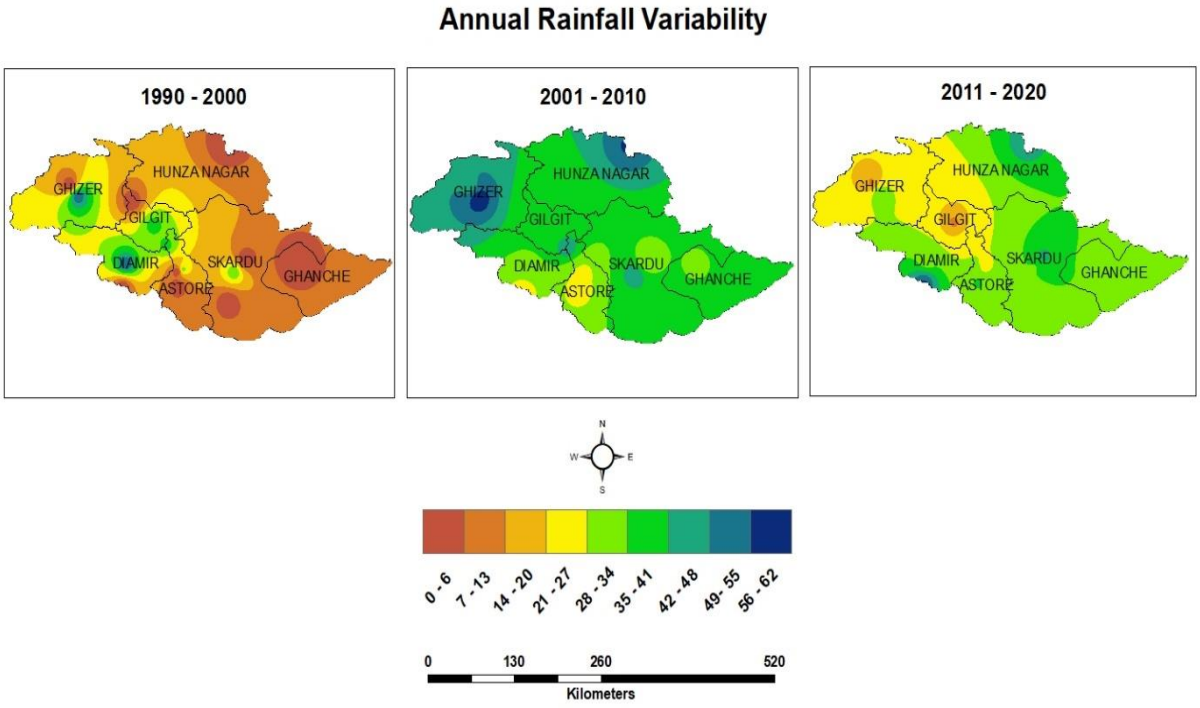

Fig. 3.13 Decadal variability in Gilgit Baltistan.

4.3 Initial Screening of the Data

4.3.1 Lag-1 Correlation Coefficient

The results of the Lag-1 correlation coefficient are shown in table 3.2 to verify for the presence of serial correlation at provided sites. For the hypothesis test of the correlation coefficient being zero, the associated P values suggest that there is no evidence of serial correlation in the data series at any point.

4.3.2 Test of randomness

The run test has been applied to assess the randomness of the data series at the selected sites (Table 3.2). The associated P values of ONR (observed number of runs) for each location demonstrate that the hypothesis of data series randomness cannot be rejected at the 5% level of significance.

4.3.3 Mann-Whitney Test

The data series at each location has been categorized into two groups to perform the Mann-Whitney test (Table 3.2). The matching P values of the test statistic indicate that there is insufficient evidence to reject the hypothesis that the observed data series at each location are identically distributed at the 5% level of significance.

The results of several tests relating to the assumption of data series at certain locations utilized for regional frequency analysis have demonstrated that the data from all seven sites is suitable for further analysis.

4.4 Discordancy measure

Table 3.3 shows the overall statistics and Di values for all fifteen locations. None of the locations had a Di value larger than 3, which is the crucial value proposed by Hosking and Wallis (1997). As a result, there are no discordant sites in the area.

As the D_i values for all stations are less than the threshold, we concluded that there was no trend or outlier in any station.

4.5 Heterogeneity Measure

The heterogeneity measure H was computed for the complete collection of fifteen sites as a single region, which came out as $\mathbf{H_1 = -0.01}$, $\mathbf{H_2 = -1.67}$ and $\mathbf{H_3 = -3.17}$. These results are indicating that the region is homogenous and acceptable for further investigation.

4.6 Selection of Regional Frequency Distribution

The five candidate distributions are Generalized Pareto Distribution (GPA), Generalized Normal Distribution (GNO), Generalized Logistic Distribution (GLO), generalized Extreme Value Distribution (GEV) and Pearson Type III Distribution (PE3).

4.6.1 L-moment ratio diagram

L-moment ratio diagram for the region under consideration is shown in Figure 1, with sample L-skewness plotted against sample L-kurtosis. The region's data has often demonstrated reduced skewness and kurtosis. In Fig. 3.14, the region's average L-skewness and L-kurtosis are also displayed, the point is located on the hypothesized Pearson Type III (PE3) and Generalized Pareto Distribution (GPA) distribution curve. As a result, these two distributions appear to be well-fitting distributions for the region under investigation

Table 3. 2 Results of lag-1 orreclation coeff, run test and mann-whitney test.

Sr no.	**Stations**	**n**	r_1	**ONR**	**P value**	**Groups**	**W**	**P value**
1	Chilas	372	0.02	135	0.3	186,186	33591	0.28
2	Gilgit	372	0.17	99	0.22	186,186	33495	0.25
3	Sakardu	372	0.24	149	0.10	186,186	33767	0.37
4	Bunji	372	0.17	168	0.09	186,186	34306	0.71
5	Astore	372	0.26	132	0.60	186,186	33063	0.19
6	Gupis	372	0.16	127	0.07	186,186	32935	0.89
7	Rattu	264	0.08	92	0.06	132,132	16534	0.12
8	Rama	264	0.04	108	0.06	132,132	16554	0.16
9	Khunjerab	264	0.11	117	0.08	132,132	16543	0.13
10	Shigar	264	0.11	96	0.06	132,132	17421	0.10
11	Deosai	264	0.29	93	0.07	132,132	16738	0.91
12	Hushey	264	0.15	112	0.10	132,132	16323	0.23
13	Yasin	264	0.12	95	0.21	132,132	17032	0.60
14	Naltar	264	0.13	115	0.07	132,132	16547	0.46
15	Babusar	180	0.14	82	0.17	80,80	7893	0.47

Note: r_1 is the Lag-1 autocorrelation coefficient, ONR is observed number of runs and W is the value of Man Whitney test

Table 3. 3 Results of l-moments and discordancy measure.

S. No.	**Sites**	**N**	**Mean**	t	t_3	t_4	D_i
1	Chilas	372	16.07204	0.630302	0.443837	0.222168	0.72
2	Gilgit	372	11.87984	0.593023	0.406897	0.218901	0.61
3	Sakardu	372	20.18414	0.610629	0.417553	0.177868	2.06
4	Bunji	372	13.31263	0.602451	0.429797	0.238035	0.28
5	Astore	372	38.99624	0.517578	0.352256	0.181178	0.22
6	Gupis	372	20.28414	0.658263	0.500722	0.299386	1.43
7	Rattu	264	34.16682	0.532817	0.346014	0.15406	0.63
8	Rama	264	28.17083	0.543926	0.380117	0.185745	0.88
9	Khunjerab	264	21.9647	0.474778	0.319416	0.195029	1.11
10	Shigar	264	24.40424	0.549728	0.375037	0.194338	0.02
11	Deosai	264	51.79739	0.431121	0.280721	0.142777	1.76
12	Hushey	264	26.50178	0.494405	0.301706	0.15139	1.28
13	Yasin	264	25.21837	0.530668	0.399861	0.244119	1.62
14	Naltar	264	23.4603	0.492935	0.332061	0.191631	0.52
15	Babusar	180	35.0935	0.503702	0.305184	0.147664	1.46

Note: N is the record length, t is the sample L-CV, t3 is the sample L-skewness and t4 is the sample L-kurtosis, D is discordancy measure.

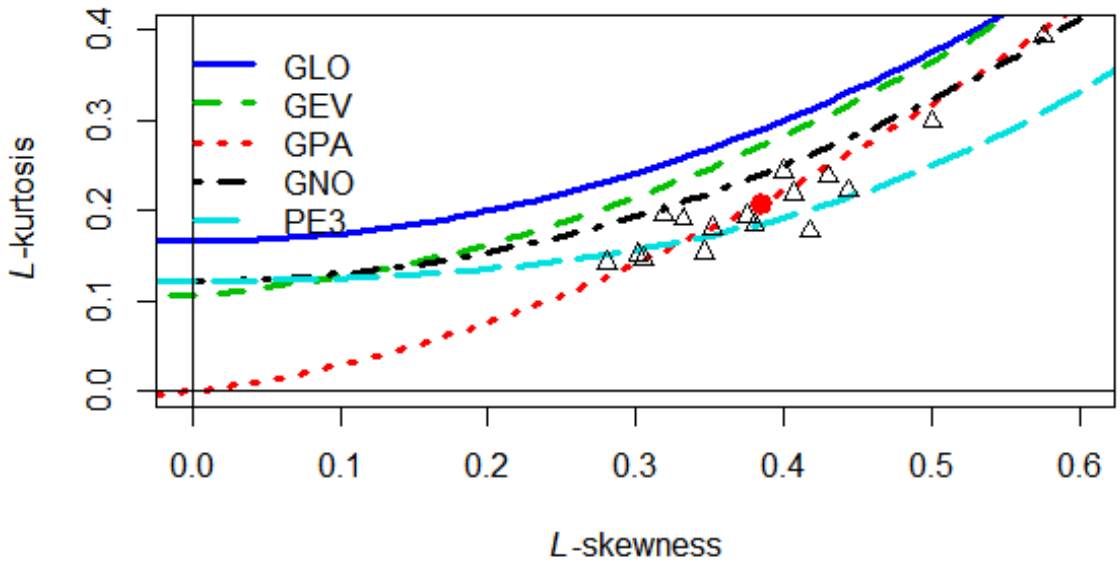

Fig. 3.14 L-moment ratio diagram of fifteen sites in Gilgit Baltistan.

Table 3. 4 Values of goodness of fit measure for different distributions.

Sr. No.	Distributions	$\lvert Z^{DIST} \rvert$
1	GLO	2.59
2	GEV	1.95
3	GNO	0.89*
4	PE3	0.94*
5	GPA	0.16*

Table 3. 5 Estimates of parameters of best fit regional distributions.

Distributions	Parameters		
	α	ε	K
GNO	0.638	0.745	-0.818
PE3	1.000	1.156	2.316
GPA	-0.050	0.933	-0.112

4.6.2 Z^{DIST} Criteria

Table 3.4 shows the measure values for the region under investigation for various parameter distributions. The goal is to obtain not only the best fit distribution for the region but also the most suitable parameter distribution for regional quantile estimation. Generalized Normal Distribution (GNO), Pearson Type III Distribution (PE3), and Generalized Pareto Distribution (GPA) all have $|Z^{DIST}|$ measure scores of less than 1.64, indicating that they would be good candidates for regional distribution. The fit is adequate if $|Z^{DIST}|$ is sufficiently close to zero. Since the Generalized Pareto Distribution (GPA) distribution has the $|Z^{DIST}|$ measure value closest to zero making it the most suitable for the region. The $|Z^{DIST}|$statistic's results were in good agreement with the L-moment ratio diagram.

4.7 Estimation of Parameters and Quantiles of Regional Distributions

Estimation parameters include α, ε and κ, which are scale parameter, location parameter and is shape parameter of the distributions respectively. (Table 3.5).

The quantiles of regional distributions are estimated for the most suitable distribution i.e., GPA, for different non-exceedance probability F and corresponding return periods T (Table 3.6). The quantile values can be interpreted as $q_{GPA}(50) = 4.529$ is the amount of rainfall that will occur once every 50 years, i.e., the probability of occurrence in any year for the given return period of 50 years is 4.529 times greater than the average for all stations in a homogeneous region for the given return period.

At-site quantiles are estimated by multiplication of site specific average annual maximum rainfall with the calculated regional quantiles to generate the appropriate rainfall quantiles for the relevant station using the regional parameters for the similar distribution at different return periods. (Table 3.7).

The stations of Astore, Naltar, Rattu, Rama, Khunjerab and Hushey have observed maximum total rainfall comparable to the calculated maximum quantiles of 100 years return period. Hence, Astore, Naltar, Rattu, Rama, Khunjerab and Hushey are expected to be at risk of facing extreme rainfall events in future as the extreme events of almost same magnitude have occurred in past three decades in these stations, which means a similar rainfall event is expected in any of the coming year with the probability of 1%. The maxima of all six stations are shown in the Table 3.8.

Moreover, out of these six sites the sites of Khunjerab, Hushey, Rama and Rattu are vulnerable to extreme rainfall event of magnitude corresponding to 100-yr return period as such events have triggered floods and other related disasters because of such events. Table 3.8 shows the historic flood events in specified regions. In September 2014 Hushey has experienced an extreme rainfall event of magnitude 144 mm and Khunjerab observed 122 mm in November 2014, as well as the whole northeastern region of Pakistan has experienced high rainfall events for several days as a result of which high flood discharges built in rivers of Chenab, Jhelum, and Ravi in Sep 2014.

In 2017 Rama station in Gilgit Baltistan has observed the rainfall event of 180 mm in January and several high seasonal rainfall spells occurred locally in Northern regions that generated flash flooding, landslides, and avalanches in Gilgit-Baltistan, KPK and sub-mountainous regions.

Moreover, the station of Rama in November 2019 experienced extreme event of 160 mm and several other northeastern regions have also experienced seasonal rainfall extreme events, that caused local events of landslides and mudflows as reported.

Table 3. 6 Reginal quantile estimates at different return periods.

Return Period	**2**	**5**	**10**	**20**	**50**	**100**
GNO	0.638	1.541	2.326	3.226	4.615	5.836
PE3	0.604	1.638	2.470	3.322	4.469	5.346
GPA	0.622	1.595	2.400	3.270	4.529	5.571

Table 3. 7 At-site rainfall distribution at different return periods.

Return Period	2	5	10	20	50	100
Chilas	10.00	25.63	38.57	52.56	72.79	89.54
Gilgit	7.39	18.95	28.51	38.85	53.80	66.18
Sakardu	12.55	32.19	48.44	66.00	91.41	112.45
Bunji	8.28	21.23	31.95	43.53	60.29	74.16
Astore	24.26	62.20	93.59	127.52	176.61	217.25
Gupis	12.62	32.35	48.68	66.33	91.87	113.00
Naltar	14.59	37.42	56.30	76.72	106.25	130.70
Rattu	21.25	54.50	82.00	111.73	154.74	190.34
Rama	17.52	44.93	67.61	92.12	127.59	156.94
Khunjerab	13.66	35.03	52.72	71.82	99.48	122.37
Shigar	15.18	38.92	58.57	79.80	110.53	135.96
Deosai	32.22	82.62	124.31	169.38	234.59	288.56
Hushey	16.48	42.27	63.60	86.66	120.03	147.64
Yasin	15.69	40.22	60.52	82.46	114.21	140.49
Babusar	21.83	55.97	84.22	114.76	158.94	195.51

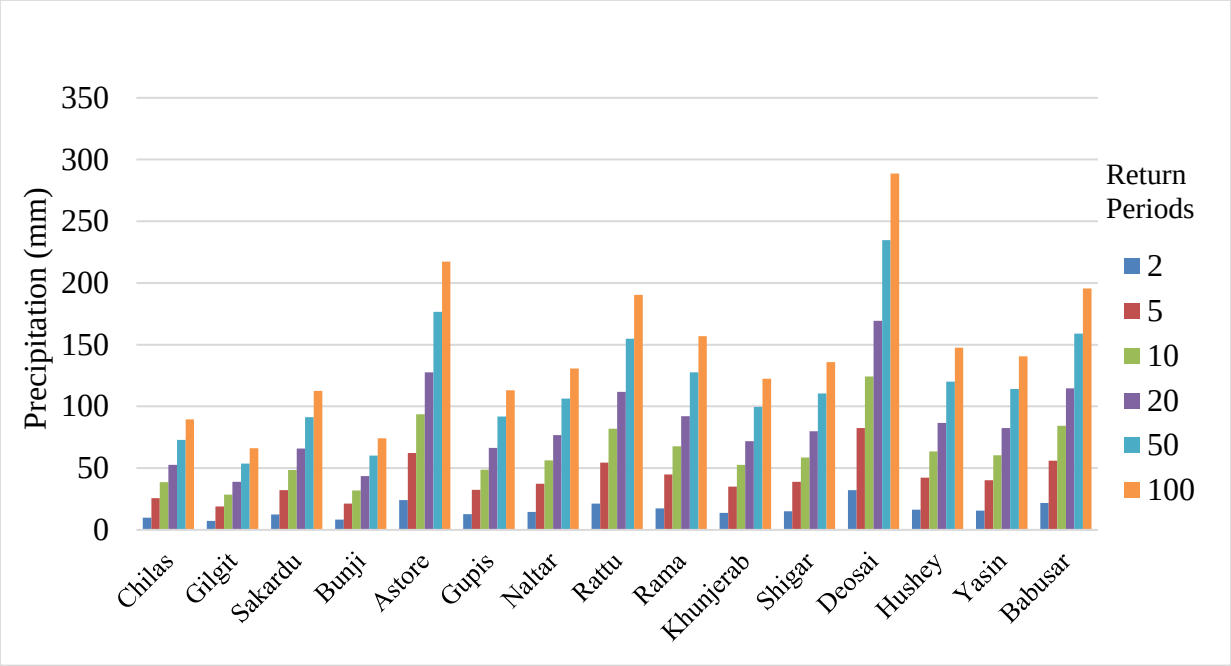

Fig. 3.15 At-site rainfall quantiles of fifteen sites in Gilgit Baltistan.

Table 3.8 Observed and calculated maxima of total rainfall.

Stations	**Astore**	**Naltar**	**Hushey**	**Khunjerab**	**Rama**	**Rattu**
Dates	Apr 1999	Apr 1999	Sep 2014	Nov 2014	Nov 2019	Jan 2017
Observed Maxima	221.2	144.13	144.32	122.8	158.83	180.2
Quantile at 100-year T	217.25	130.7	147.64	122.37	156.94	190.34

Chapter 5

CONCLUSION AND RECOMMENDATIONS

The result of the study shows that 37% of annual precipitation of Gilgit Baltistan is recorded in Pre-monsoon season in last three decades. Whereas 26.5% and 25.4% of annual precipitation is recorded in Winters and Monsoon seasons. Since, most of the precipitation in Northern regions of Pakistan is due to westerlies hence the rainy season is winters in Gilgit Baltistan.

Moreover, most of the stations showed insignificant trends of rainfall. Astore is the only station in study area where precipitation has decreased by 186 (mm) over past three decades whereas in Khunjerab and Hushey, it has increased by 230 (mm) and 252 (mm) in last two decades. In Babusar and Khunjerab, precipitation has increased by 27 (mm) and 12 (mm) in monsoon respectively. And in Winters, precipitation in Babusar has decreased by 41 (mm).

Furthermore, the study is conducted on the fifteen sites of Gilgit Baltistan for the annual monthly total precipitation estimates for different return periods. Linear moments are calculated and as per the heterogeneity measure, whole region of Gilgit Baltistan is homogeneous to work further. Based on L-moments, five probability distributions are selected i.e., Generalized Pareto Distribution (GPA), Generalized Normal Distributions (GNO), Generalized Logistic Distribution (GLO), Generalized extreme value (GEV) and Pearson Type III (PE3). Generalized pareto Distribution (GPA) is appeared to be the most suitable distribution for the data, out of all five selected distributions. The selection is done by the L-moments ratio diagram technique and Z-statistics criteria. Rainfall regional quantiles and at-site quantiles are estimated.

Generally, the precipitation quantiles are increasing with the increased return periods. Among the fifteen stations in GB, the stations of Astore, Naltar, Rattu, Rama, Khunjerab and Hushey are expected to be at risk of facing extreme rainfall events in future as the extreme events of almost same magnitude have occurred in past three decades in these stations. Hence, these stations are at higher risk of observing 100 years return period event in any of coming year with 1% probability.

Moreover, according to Annual Flood Report of 2014, 2017 and 2019, seasonal and torrential rainfall spells triggered floods, landslides, mudflows etc., in specific area of country including several regions in Gilgit Baltistan. This makes the sites of Hushey, Khunjerab, Rama and Rattu vulnerable to extreme rainfall events in future.

These annual monthly total rainfall quantiles at different sites distributed all over the northern region of Pakistan might be utilized for hydrological planning and management of water resources in the future especially for the sites at higher risk, notably during pre-monsoon times as the highest amount of rainfall in Gilgit Baltistan occurs in pre-monsoon season. The estimated rainfall quantiles could be employed by researchers, scientists, hydrologists, government authorities for flood disaster prevention, agricultural water management, and improvement projects for main barrages, Dams and spillways renovation.

REFERENCES

Ahmad, ishfaq, Fawad, M., & Mahmood, I. (2015). At-Site Flood Frequency Analysis of Annual Maximum Stream Flows in Pakistan Using Robust Estimation Methods. *Polish Journal of Environmental Studies*, *24*(6), 2345–2353. https://doi.org/10.15244/pjoes/59585

Ahmad, I., Abbass, A., Fawad, M., & Saghir, A. (2017). Regional Frequency Analysis of Annual Total Rainfall in Pakistan Using L- Moments. *NUST Journal of Engineering Sciences (NJES)*, *10*(1), 19–29.

Aihaiti, A., Jiang, Z., Zhu, L., Li, W., & You, Q. (2021). Risk changes of compound temperature and precipitation extremes in China under 1.5 °C and 2 °C global warming. *Atmospheric Research*, *264*. https://doi.org/10.1016/j.atmosres.2021.105838

Ali, S., Ajmal, M., Khan, M. S., & Shah, S. U. (2017). Assessment of precipitation trends in Gilgit Baltistan (Pakistan) for the period 1980-2015: An indicator of climate change. *Journal of Himalayan Earth Sciences*, *50*(1), 66–75.

Asfaw, A., Simane, B., Hassen, A., & Bantider, A. (2018). Variability and time series trend analysis of rainfall and temperature in northcentral Ethiopia: A case study in Woleka sub-basin. *Weather and Climate Extremes*, *19*, 29–41. https://doi.org/10.1016/j.wace.2017.12.002

Asong, Z. E., Khaliq, M. N., & Wheater, H. S. (2015). Regionalization of precipitation characteristics in the Canadian Prairie Provinces using large-scale atmospheric covariates and geophysical attributes. *Stochastic Environmental Research and Risk Assessment*, *29*(3), 875–892. https://doi.org/10.1007/s00477-014-0918-z

Gedefaw, M., Yan, D., Wang, H., Qin, T., Girma, A., Abiyu, A., & Batsuren, D. (2018). Innovative trend analysis of annual and seasonal rainfall variability in Amhara Regional State, Ethiopia. *Atmosphere*, *9*(9). https://doi.org/10.3390/atmos9090326

Hansen, C. R. (2015). Comparison of regional and at-site frequency analysis methods for the estimation of southern Alberta extreme rainfall. *Canadian Water Resources Journal*, *40*(4), 325–342. https://doi.org/10.1080/07011784.2015.1060871

Hoegh-Guldberg, O., Jacob, D., & Taylor, M. (2018). Impacts of 1.5°C of Global Warming on Natural and Human Systems. *Special Report, Intergovernmental Panel on Climate Change, ISBN 978-92-9169-151-7*, 175–181. http://report.ipcc.ch/sr15/pdf/sr15_chapter3.pdf

Hussain, F., Nabi, G., & Wu, R. S. (2021). Spatiotemporal Rainfall Distribution of Soan River Basin, Pothwar Region, Pakistan. *Advances in Meteorology*, *2021*. https://doi.org/10.1155/2021/6656732

Hussain, Z., Shahzad, M. N., & Abbas, K. (2017). Application of regional rainfall frequency analysis on seven sites of Sindh, Pakistan. *KSCE Journal of Civil Engineering*, *21*(5), 1812–1819. https://doi.org/10.1007/s12205-016-0946-y

IPCC, 2022: Climate Change 2022: Impacts, Adaptation, and Vulnerability. Contribution of Working Group II to the Sixth Assessment Report of the Intergovernmental Panel on Climate Change [H.-O. Pörtner, D.C. Roberts, M. Tignor, E.S. Poloczanska, K. Mintenbeck, A. Alegría, M. Craig, S. Langsdorf, S. Löschke, V. Möller, A. Okem, B. Rama (eds.)]. Cambridge University Press. In Press.

Journal, S., & Zealand, N. (1991). *NEW ZEALAND REGIONAL FLOOD FREQUENCY ANALYSIS USING L-MOMENTS Published by : New Zealand Hydrological Society*. *30*(2), 53–64.

Kaur, N., Yousuf, A., & Singh, M. J. (2021). Long term rainfall variability and trend analysis in lower Shivaliks of Punjab, India. *Mausam*, *72*(3), 571–582. https://doi.org/10.54302/mausam.v72i3.1307

Khan, S. A., Hussain, I., Hussain, T., Faisal, M., Muhammad, Y. S., & Mohamd Shoukry, A.

(2017). Regional Frequency Analysis of Extremes Precipitation Using L-Moments and Partial L-Moments. *Advances in Meteorology*, *2017*. https://doi.org/10.1155/2017/6954902

Lawrence, J., Blackett, P., & Cradock-Henry, N. A. (2020). Cascading climate change impacts and implications. *Climate Risk Management*, *29*. https://doi.org/10.1016/j.crm.2020.100234

Mesbahzadeh, T., Soleimani Sardoo, F., & Kouhestani, S. (2019). Flood frequency analysis for the Iranian interior deserts using the method of L-moments: A case study in the Loot River Basin. *Natural Resource Modeling*, *32*(2), 1–14. https://doi.org/10.1111/nrm.12208

Nain, M., & Hooda, B. K. (2021). Regional Frequency Analysis of Maximum Monthly Rainfall in Haryana State of India Using L-Moments. *Journal of Reliability and Statistical Studies*, *14*(1), 33–56. https://doi.org/10.13052/jrss0974-8024.1413

Nair, A., Ajith Joseph, K., & Nair, K. S. (2014). Spatio-temporal analysis of rainfall trends over a maritime state (Kerala) of India during the last 100 years. *Atmospheric Environment*, *88*, 123–132. https://doi.org/10.1016/j.atmosenv.2014.01.061

Rahman, M. R., & Lateh, H. (2017). Climate change in Bangladesh: a spatio-temporal analysis and simulation of recent temperature and rainfall data using GIS and time series analysis model. *Theoretical and Applied Climatology*, *128*(1–2), 27–41. https://doi.org/10.1007/s00704-015-1688-3

Reiter, A., Weidinger, R., & Mauser, W. (2012). Recent Climate Change at the Upper Danube-A temporal and spatial analysis of temperature and precipitation time series. *Climatic Change*, *111*(3), 665–696. https://doi.org/10.1007/s10584-011-0173-y

Shehzad Hasan Shigri, K. H. (2017). *Gilgit-Baltistan Climate Change Strategy and Action Plan*.

Tabari, H. (2020). Climate change impact on flood and extreme precipitation increases with water availability. *Scientific Reports*, *10*(1), 1–10. https://doi.org/10.1038/s41598-020-70816-2

Trewin, B., Cazenave, A., Howell, S., Huss, M., Isensee, K., Palmer, M. D., Tarasova, O., & Vermeulen, A. (2021). Headline indicators for global climate monitoring. *Bulletin of the American Meteorological Society*, *102*(1), E20–E37. https://doi.org/10.1175/BAMS-D-19-0196.1

World Meteorological Organization. (2022). *State of the Global Climate 2021*. *WMO-No. 1290*, 1–56.

Yin, Y., Chen, H., Xu, C. Y., Xu, W., Chen, C., & Sun, S. (2016). Spatio-temporal characteristics of the extreme precipitation by L-moment-based index-flood method in the Yangtze River Delta region, China. *Theoretical and Applied Climatology*, *124*(3–4), 1005–1022. https://doi.org/10.1007/s00704-015-1478-y